Muon anomalous magnetic moment, lepton flavor violation, and flavor changing neutral current processes in supersymmetric grand unified theory with right-handed neutrinos

Seungwon Baek,[1] Toru Goto,[2] Yasuhiro Okada,[2,3] and Ken-ichi Okumura[4]
[1]*Department of Physics, National Taiwan University, Taipei 106, Taiwan*
[2]*Theory Group, KEK, Tsukuba, Ibaraki, 305-0801 Japan*
[3]*Department of Particle and Nuclear Physics, The Graduate University of Advanced Studies, Tsukuba, Ibaraki, 305-0801 Japan*
[4]*Institute for Cosmic Ray Research, University of Tokyo, Kashiwanoha 5-1-5, Kashiwa, 277-8582 Japan*
(Received 16 April 2001; published 12 September 2001)

Motivated by the large mixing angle solutions for the atmospheric and solar neutrino anomalies, flavor changing neutral current processes and lepton flavor violating processes as well as the muon anomalous magnetic moment are analyzed in the framework of SU(5) supersymmetric grand unified theory (SUSY GUT) with right-handed neutrinos. In order to explain realistic mass relations for quarks and leptons, we take into account the effects of higher dimensional operators above the GUT scale. It is shown that the supersymmetric contributions to the CP violation parameter in K^0-$\overline{K^0}$ mixing, ε_K, the $\mu \to e\,\gamma$ branching ratio, and the muon anomalous magnetic moment become large in a wide range of parameter space. We also investigate the correlations among these quantities. Within the current experimental bound of $B(\mu \to e\,\gamma)$, large SUSY contributions are possible either in the muon anomalous magnetic moment or in ε_K. In the former case, the favorable value of the recent muon anomalous magnetic moment measurement at the BNL E821 experiment can be accommodated. In the latter case, the allowed region of the Kobayashi-Maskawa phase can be different from the prediction within the standard model (SM) and therefore measurements of the CP asymmetry of the $B \to J/\psi K_S$ mode and Δm_{B_s} could discriminate this case from the SM. We also show that the $\tau \to \mu\,\gamma$ branching ratio can be close to the current experimental upper bound and the mixing induced CP asymmetry of the radiative B decay can be enhanced in the case where the neutrino parameters correspond to the Mikheyev-Smirnov-Wolfenstein small mixing angle solution.

DOI: 10.1103/PhysRevD.64.095001 PACS number(s): 12.60.Jv, 11.30.Fs, 13.20.He, 14.60.Pq

I. INTRODUCTION

In order to explore physics beyond the standard model (SM), indirect searches play an important role complimentary to direct searches for new particles at high energy frontiers. The indirect searches include flavor changing neutral current (FCNC) processes, lepton flavor violation (LFV), and the muon anomalous magnetic moment. In the minimal SM, lepton flavor is conserved and FCNC is forbidden at the tree level, so that B, K, and μ decay experiments have supplied severe constraints on models beyond the SM. At the recent BNL E821 experiment, it was reported that the muon anomalous magnetic moment had a 2.6σ deviation from the SM prediction [1]. If the deviation is confirmed by improvements in both statistics and understanding of the theoretical uncertainty of the SM prediction, the muon anomalous magnetic moment will become a clear signal of physics beyond the SM.

Among candidates for physics beyond the SM, supersymmetry (SUSY) is the most attractive one. Because of the cancellation of quadratic divergence in the renormalization of the Higgs field, SUSY models do not have the hierarchy problem of the SM. Furthermore, gauge coupling unification is realized in SUSY grand unified theories (SUSY GUT) based on the SU(5) gauge group or its extensions.

In view of flavor physics, it is important that the scalar partners of quarks and leptons, namely, squarks and sleptons, have a new source of flavor mixing. Because of the new flavor mixing, LFV and FCNC such as $\mu \to e\,\gamma$, $b \to s\,\gamma$, and K^0-$\overline{K^0}$/B^0-$\overline{B^0}$ mixing could be induced through SUSY loop diagrams. Because these processes receive contributions too large for generic flavor mixing in the squark and slepton sectors, the structure of the SUSY breaking sector of the Lagrangian is required to have a special form, unless the masses of the SUSY particles are beyond the multi-TeV region [2]. The simplest possibility to avoid this problem is that the SUSY breaking mechanism is assumed to be flavor blind. However, even in such a case, the squark and slepton mass matrices receive radiative corrections from interactions below the scale where the SUSY breaking is originated, and flavor blindness is broken [3,4]. In particular, effects of the large top Yukawa coupling constant cannot be neglected. A number of analyses have been done in the context of the minimal supergravity (minimal SUGRA) ansatz where SUSY breaking parameters are assumed to be flavor blind at the Planck scale [5–8]. It was shown that the flavor mixing is controlled by the Cabibbo-Kobayashi-Maskawa (CKM) matrix element. As a result the maximal deviation from the SM in the CP violating parameter of K^0-$\overline{K^0}$ mixing, ε_K, and B_d-$\overline{B_d}$/B_s-$\overline{B_s}$ mixing is of the order of 10%, while the SUSY contribution to the $b \to s\,\gamma$ process can be very important [7,8]. In the GUT scenario, there are additional contributions to FCNC-LFV processes from GUT interactions [4,9–12]. As for LFV processes the $\mu \to e\,\gamma$ branching ratio is close to the current experimental bound, especially for the SO(10) model [10].

Recent experimental evidence of neutrino oscillation indicates the existence of small neutrino mass and large flavor

mixing in the lepton sector [13]. A natural explanation for the small neutrino mass is the seesaw mechanism [14]. In this mechanism, heavy right-handed neutrinos are introduced, and these neutrinos have a Majorana mass term and new Yukawa interactions. Because the neutrino Yukawa coupling constants can be as large as the top Yukawa coupling constant if the right-handed neutrinos are $O(10^{14})$ GeV, radiative corrections from these interactions contribute to the renormalization of the slepton mass matrix above the mass scale of the right-handed neutrinos. Within the minimal SUGRA scenario, it was shown that the branching ratios of LFV processes become large enough to be measured in near-future experiments [15–17]. Some GUT models that have predictable neutrino mass and mixing are already constrained [18]. In the context of SUSY GUT, these new interactions in the lepton sector also contribute to the quark sector, because radiative corrections on the squark from neutrino interactions can become a new source of quark FCNC processes as well as LFV processes. Recently, these processes were analyzed in the minimal SU(5) SUSY GUT with right-handed neutrinos, and large deviations from the SM were predicted [19,20]. However, in these analyses, simple flavor structure was assumed so that the correct mass relations between the down-type quarks and charged leptons in the first and second generations cannot be realized.

Very recently, the BNL E821 experiment reported a new result on the muon anomalous magnetic moment [1]. The measured value of $a_\mu=(g_\mu-2)/2$ is $a_\mu(\text{expt})=11659202(14)(6)\times10^{-10}$, which compares to the SM prediction $a_\mu(\text{SM})=11659159.6(6.7)\times10^{-10}$. It was concluded that the theory and experiment had a 2.6σ difference $a_\mu(\text{expt})-a_\mu(\text{SM})=43(16)\times10^{-10}$. The deviation can be explained in the context of the SUSY model [21]. In contrast to the LFV and FCNC processes, which are very sensitive to the origin of the flavor mixing at high energy scale, the muon anomalous magnetic moment can provide us with information on the slepton masses, independent of the flavor structure of the slepton mass matrices.

In this paper, we discuss FCNC/LFV processes in SU(5) supersymmetric grand unified theory with right-handed neutrinos [SU(5)RN SUSY GUT] taking account of realistic mass relations. The seesaw mechanism generates small neutrino masses and large mixing angles which incorporate atmospheric and solar neutrino anomalies. In order to reproduce realistic mass relations, we introduce a higher dimensional operator including a **24** superfield which gives contributions to the Yukawa coupling matrices for the down-type quarks and the charged leptons in a different manner. Moreover, new degrees of freedom arise in the choice of the bases when minimal supersymmetric standard model (MSSM) multiplets are embedded in SU(5) multiplets. We show that the main effect of these new mixings is described by two mixing angles that parametrize rotations of the bases between the down-type quarks and charged leptons in the first and second generations. We perform numerical analysis on FCNC/LFV processes taking account of various sources of flavor mixing. We also calculate the muon anomalous magnetic moment and investigate the correlations among these quantities. Solving renormalization group equations for the Yukawa coupling matrices and the SUSY breaking parameters, the flavor mixing in the squark and slepton sectors is evaluated at the electroweak (EW) scale. In addition to the muon anomalous magnetic moment, we calculate the following FCNC/LFV observables: the branching ratios of $\mu\to e\,\gamma$, $\tau\to\mu\,\gamma$, and $b\to s\,\gamma$, ε_K, the mass differences in B_d-$\overline{B}_d$ mixing and B_s-$\overline{B}_s$ mixing, and the time-dependent CP asymmetries of $B\to J/\psi K_S$ and $B\to M_s\,\gamma$ where M_s is a CP eigenstate including a strange quark. We find that the SUSY contributions to ε_K, the $\mu\to e\,\gamma$ branching ratio, and the muon anomalous magnetic moment become large in a wide range of parameter space. Within the current experimental bound on $B(\mu\to e\,\gamma)$, large SUSY contributions are possible either in the muon anomalous magnetic moment or in ε_K. In the former case, the favorable value of the recent muon anomalous magnetic moment measurement at the BNL experiment can be accommodated. In the latter case, the new contribution ε_K modifies the constraint for the CKM matrix elements and affects B decay observables because the allowed region of $\Delta m_{B_s}/\Delta m_{B_d}$ and the time-dependent CP asymmetry of the $B\to J/\psi K_S$ mode can be quite different from those of the SM or MSSM without the new flavor mixing source. We also show that $B(\tau\to\mu\,\gamma)$ and the indirect CP asymmetry of the radiative B decay can be large in the case where the neutrino parameters correspond to the small mixing angle Mikheyev-Smirnov-Wolfenstein (MSW) solution. We also notice that the branching ratio of $\mu\to e\,\gamma$ can be close to the present experimental upper limit in both the large and small mixing angle MSW solutions.

The rest of this paper is organized as follows. In Sec. II, the SU(5)RN SUSY GUT is introduced. The higher dimensional operators are included to incorporate a realistic fermion mass relation. Two new mixing angles are defined to parametrize the effect of these operators. In Sec. III, the minimal SUGRA model is introduced for the SUSY breaking sector. Radiative corrections for the SUSY breaking parameters and FCNC/LFV processes are discussed qualitatively using approximate formulas. In Sec. IV, the numerical results for the muon anomalous magnetic moment and FCNC/LFV processes are presented. Section V is devoted to conclusions and discussion. In the Appendixes, useful formulas are collected.

II. SU(5) SUSY GUT WITH RIGHT-HANDED NEUTRINO

In this section we discuss quark and lepton Yukawa couplings in the SU(5)RN SUSY GUT. Before introducing higher dimensional operators, we first discuss the case without them. Later, we introduce those operators to accommodate a realistic mass relation. Without higher dimensional operators, the Yukawa coupling and the Majorana mass term of the superpotential for this model are given by

$$\begin{aligned}\mathcal{W}_{\text{SU(5)RN}}=&\frac{1}{8}\epsilon_{abcde}(\lambda_u)_{ij}(T^i)^{ab}(T^j)^{cd}H^e\\&+(\lambda_d)_{ij}(\overline{F}^i)_a(T^j)^{ab}\overline{H}_b+(\lambda_\nu)_{ij}\overline{N}^i(\overline{F}^j)_aH^a\\&+\frac{1}{2}(M_\nu)_{ij}\overline{N}^i\overline{N}^j,\end{aligned}\tag{1}$$

where T^i, $\overline{F}^i$, and $\overline{N}^i$ are the **10**, $\overline{\mathbf{5}}$, and **1** representations of the SU(5) gauge group, respectively. i,j are generation indices and a, b, c, d, and e are SU(5) indices. ϵ_{abcde} is the totally antisymmetric tensor of the SU(5) gauge group. H and $\overline{H}$ are Higgs superfields with **5** and $\overline{\mathbf{5}}$ representations. In terms of $\mathrm{SU}(3)\times\mathrm{SU}(2)_L\times\mathrm{U}(1)_Y$, T^i contains $Q^i(\mathbf{3},\mathbf{2},\frac{1}{6})$, $\overline{U}^i(\overline{\mathbf{3}},\mathbf{1},-\frac{2}{3})$, and $\overline{E}^i(\mathbf{1},\mathbf{1},1)$ superfields. Here the representations for SU(3) and SU(2) groups and the $U(1)_Y$ charge are indicated in parentheses. $\overline{F}^i$ includes $\overline{D}^i(\mathbf{3},\mathbf{1},\frac{1}{3})$ and $L^i(\mathbf{1},\mathbf{2},-\frac{1}{2})$, and $\overline{N}^i$ is a singlet of $\mathrm{SU}(3)\times\mathrm{SU}(2)_L\times\mathrm{U}(1)_Y$. H consists of $H_C(\mathbf{3},\mathbf{1},0)$ and $H_2(\mathbf{1},\mathbf{2},\frac{1}{2})$ and $\overline{H}$ contains $\overline{H}_C(\overline{\mathbf{3}},\mathbf{1},0)$ and $H_1(\mathbf{1},\mathbf{2},-\frac{1}{2})$. $(\lambda_u)_{ij}$, $(\lambda_d)_{ij}$, and $(\lambda_\nu)_{ij}$ are Yukawa coupling matrices and $(M_\nu)_{ij}$ is a Majorana mass matrix. In addition to the above formula, we also need a superpotential for Higgs superfields, $\mathcal{W}_H(H,\overline{H},\Sigma)$, where Σ^a_b is a **24** representation of the SU(5) group. It is assumed to develop vacuum expectation values as $\langle\Sigma^a_b\rangle=\mathrm{diag}(\frac{1}{3},\frac{1}{3},\frac{1}{3},-\frac{1}{2},-\frac{1}{2})v_G$ at the GUT scale ($M_G\approx 2\times 10^{16}$ GeV) and breaks the SU(5) symmetry to $\mathrm{SU}(3)\times\mathrm{SU}(2)_L\times\mathrm{U}(1)_Y$.

Below the GUT scale, the heavy superfields such as H_C, $\overline{H}_C$, and Σ are integrated out and the superpotential of the MSSM with right-handed neutrino (MSSMRN) is given by

$$\mathcal{W}_{\mathrm{MSSMRN}}=(y_u)_{ij}\overline{U}^iQ^jH_2+(y_d)_{ij}\overline{D}^iQ^jH_1+(y_e)_{ij}\overline{E}^iL^jH_1+(y_\nu)_{ij}\overline{N}^iL^jH_2+\frac{1}{2}(M_\nu)_{ij}\overline{N}^i\overline{N}^j+\mu H_1H_2, \quad (2)$$

where Yukawa coupling matrices are related to those of the SU(5)RN model as $(y_u)_{ij}=(\lambda_u)_{ij}$, $(y_d)_{ij}=(y_e^T)_{ij}=(\lambda_d)_{ij}$, and $(y_\nu)_{ij}=(\lambda_\nu)_{ij}$. Below the Majorana mass scale ($\equiv M_R$), the singlet fields are also integrated out from the superpotential and a dimension five operator is generated as follows:

$$\Delta\mathcal{W}_\nu=-\frac{1}{2}(K_\nu)_{ij}(L_iH_2)(L_jH_2),$$

$$K_\nu=(y_\nu^T)_{ik}\left(\frac{1}{M_\nu}\right)^{kl}(y_\nu)_{lj}. \quad (3)$$

After the EW symmetry breaking, this operator induces by the seesaw mechanism the following neutrino mass matrix:

$$(m_\nu)_{ij}=(K_\nu)_{ij}\langle H_2\rangle^2. \quad (4)$$

In this model, the naive GUT relation is predicted at the GUT scale,

$$(y_e)_{ij}=(y_d)_{ji}. \quad (5)$$

Although this relation gives a reasonable agreement for m_b and m_τ, it is well known that the mass ratio of down-type quarks and charged leptons in the first and second generations cannot be explained in this way. One possibility to remedy this defect is to introduce higher dimensional operators above the GUT scale because they can give different contributions to the Yukawa coupling matrices of down-type quarks and charged leptons after the SU(5) symmetry breaking.

We consider higher dimensional operators including the **24** Higgs superfield up to dimension five terms. Relevant parts of the superpotential are parametrized as follows:

$$\begin{aligned}\Delta\mathcal{W}_{\mathrm{SU(5)RN}}=\frac{1}{M_X}\Big[&\frac{1}{4}\epsilon_{abcde}(\kappa_u^+)_{ij}\{\Sigma^a{}_f(T^i)^{fb}(T^j)^{cd}+(T^i)^{ab}\Sigma^c{}_f(T^j)^{fd}\}H^e\\&+\frac{1}{4}\epsilon_{abcde}(\kappa_u^-)_{ij}\{\Sigma^a{}_f(T^i)^{fb}(T^j)^{cd}-(T^i)^{ab}\Sigma^c{}_f(T^j)^{fd}\}H^e\\&+(\kappa_d)_{ij}(\overline{F}^i)_a\Sigma^a{}_b(T^j)^{bc}\overline{H}_c+(\overline{\kappa}_d)_{ij}(\overline{F}^j)_a(T^j)^{ab}\Sigma^c{}_b\overline{H}_c\\&+(\kappa_\nu)_{ij}\overline{N}^i(\overline{F}^j)_a\Sigma^a{}_bH^b\Big],\end{aligned} \quad (6)$$

where M_X is the cutoff scale, which we take as the Planck mass M_P. We also assume that the elements of coupling matrices $\kappa_u^\pm$, κ_d, $\overline{\kappa}_d$, and κ_ν are smaller than $O(1)$. After SU(5) symmetry is broken, they give contributions of the order of $\xi=v_G/M_X\approx 0.01$ to the Yukawa coupling constants of the MSSMRN as follows:

$$(y_u)_{ij}=(\lambda_u)_{ij}+\xi\left\{\frac{1}{2}(\kappa_u^+)_{ij}+\frac{5}{6}(\kappa_u^-)_{ij}\right\}, \quad (7a)$$

$$(y_d)_{ij}=(\lambda_d)_{ij}+\xi\left\{\frac{1}{3}(\kappa_d)_{ij}-\frac{1}{2}(\overline{\kappa}_d)_{ij}\right\}, \quad (7b)$$

$$(y_e)_{ij}=(\lambda_d^T)_{ij}+\xi\left\{-\frac{1}{2}(\kappa_d^T)_{ij}-\frac{1}{2}(\overline{\kappa}_d^T)_{ij}\right\}, \quad (7c)$$

$$(y_\nu)_{ij}=(\lambda_\nu)_{ij}-\frac{\xi}{2}(\kappa_\nu)_{ij}. \quad (7d)$$

The naive GUT relation between the lepton and the down-type quark Yukawa coupling matrices in Eq. (5) is modified to

$$(y_e)_{ij}=(y_d)_{ji}+\frac{5}{6}\xi(\kappa_d)_{ji}. \quad (8)$$

With this small contribution from the higher dimensional operator, realistic mass relations between the down-type quarks and charged leptons can be incorporated in the model. In the following analysis we take $(\kappa_u^+)_{ij}=(\kappa_u^-)_{ij}=(\overline{\kappa}_d)_{ij}=(\kappa_\nu)_{ij}=0$ because they are not necessarily required to reproduce the realistic mass relations.

In the following, we show that new mixing angles are introduced at the GUT scale because of κ_d. Using SU(5) symmetry, we can rotate the generation indices of superfields

in Eq. (2) so that the Yukawa coupling constants and the Majorana mass matrix are parametrized as follows:

$$(y_u)_{ij}=(V_{\rm CKM}^T V_U^*)_i^k y_{uk}(V_{\rm CKM})^k{}_j, \tag{9a}$$

$$(y_d)_{ij}=(V_D^*)_i{}^j y_{dj}, \tag{9b}$$

$$(y_e)_{ij}=(V_E^*)_i{}^j y_{ej}, \tag{9c}$$

$$(y_\nu)_{ij}=y_{\nu i}(V_L)^i{}_j, \tag{9d}$$

$$(M_\nu)_{ij}=(V_N^T)_i{}^k M_{\nu k}(V_N)^k{}_j, \tag{9e}$$

where V_U, V_E, V_D, and V_N are unitary matrices and $V_{\rm CKM}$ is the CKM matrix at the GUT scale. y_{ui}, y_{di}, y_{ei}, $y_{\nu i}$, and $M_{\nu i}$ represent the eigenvalues of the Yukawa coupling matrices and the Majorana mass matrix. The GUT relation between the two Yukawa coupling constants is then given by

$$(V_D^*)_i{}^j y_{dj}-y_{ei}(V_E^\dagger)^i{}_j=\frac{5}{6}\xi(\kappa_d)_{ij}. \tag{10}$$

From this formula we can derive the following approximate relations for the 1-3 and 2-3 (3-1 and 3-2) elements of the mixing matrices because the Yukawa coupling constants of the first and second generations are much smaller than that of the third generation,

$$(V_D)^i{}_3\approx\frac{5}{6}\frac{\xi}{y_b}(\kappa_d^*)_{i3}, \tag{11a}$$

$$(V_E)^i{}_3\approx-\frac{5}{6}\frac{\xi}{y_\tau}(\kappa_d^\dagger)_{i3}, \tag{11b}$$

$$(V_E)^3{}_i\approx\frac{5}{6}\frac{\xi}{y_b}(V_D^T\kappa_d V_E)_{3i}, \tag{11c}$$

$$(V_D)^3{}_i\approx-\frac{5}{6}\frac{\xi}{y_\tau}(V_E^T\kappa_d^T V_D)_{3i}, \tag{11d}$$

for $i=1,2$. We can estimate ξ/y_b and ξ/y_τ as

$$\frac{\xi}{y_b}\approx\frac{\xi}{y_\tau}\approx-\frac{\xi v\cos\beta}{\sqrt{2}m_\tau},\qquad \frac{v}{\sqrt{2}}=\sqrt{\langle H_1\rangle^2+\langle H_2\rangle^2}, \tag{12}$$

where β is the vacuum angle of two Higgs vacuum expectation values ($\tan\beta=\langle H_2^0\rangle/\langle H_1^0\rangle$). Assuming the condition $(\kappa_d)_{ij}\lesssim O(1)$, we can conclude that the magnitude of these elements is constrained to be smaller than $(\tan\beta)^{-1}$ because the lower $\tan\beta$ region is excluded from the Higgs boson search. On the other hand, the 1-2 (2-1) element is not constrained by such a consideration. Motivated by this observation we assume the following form:

$$(V_D)^i{}_j=e^{i\gamma_D}\begin{pmatrix} e^{i\alpha_D}\cos\theta_D & -e^{-i\beta_D}\sin\theta_D & 0\\ e^{i\beta_D}\sin\theta_D & e^{-i\alpha_D}\cos\theta_D & 0\\ 0 & 0 & e^{i(-\gamma_D+\delta)}\end{pmatrix}, \tag{13a}$$

$$(V_E)^i{}_j=e^{i\gamma_E}\begin{pmatrix} e^{i\alpha_E}\cos\theta_E & -e^{-i\beta_E}\sin\theta_E & 0\\ e^{i\beta_E}\sin\theta_E & e^{-i\alpha_E}\cos\theta_E & 0\\ 0 & 0 & e^{i(-\gamma_E+\delta)}\end{pmatrix}. \tag{13b}$$

The antisymmetric part of the Yukawa matrix for the up-type quarks is also written by the coefficients of the dimension five operator as follows:

$$(V_U^*)_i{}^j y_{uj}-y_{ui}(V_U^\dagger)^i{}_j=\frac{5}{6}\xi(V_{\rm CKM}^*\kappa_u^- V_{\rm CKM}^\dagger)_{ij}. \tag{14}$$

Because we set $(\kappa_u^-)_{ij}=0$ for simplicity, $(V_U)^i{}_j$ becomes $e^{i\phi_{Ui}}\delta^i{}_j$ in our analysis.

The neutrino Yukawa coupling matrix and the Majorana mass matrix are constrained by the oscillation solutions of the atmospheric and solar neutrino anomalies. In the basis where the charged lepton mass matrix is diagonal, the neutrino mass matrix is written as follows:

$$(m_\nu)_{ij}=(V_{\rm MNS}^*)_i{}^k m_{\nu k}(V_{\rm MNS}^\dagger)^k{}_j, \tag{15}$$

where $V_{\rm MNS}$ is the Maki-Nakagawa-Sakata (MNS) matrix [22]. At the Majorana mass scale Eqs. (3) and (4) are solved as follows:

$$(V_N^*)_i{}^k y_{\nu k}(V_L)^k{}_j=\frac{1}{\langle H_2\rangle}\sqrt{M_{\nu i}}(O_\nu^T)_i{}^k\sqrt{m_{\nu k}}(V_{\rm MNS}^\dagger)^k{}_j, \tag{16}$$

where O_ν is a complex orthogonal matrix that cannot be determined from the low energy experiments. Although we neglect the running effect of the neutrino mass matrix between the low energy scale and the GUT scale in Eqs. (15) and (16), later we fully take account of this effect in the numerical calculation in Sec. IV.

III. MINIMAL SUGRA, THE MUON ANOMALOUS MAGNETIC MOMENT, AND FCNC/LFV PROCESSES

In Sec. III A we first discuss the flavor mixing of squark and slepton mass matrices induced by the radiative correction due to the Yukawa coupling constants. In order to explain qualitative features we show the one-loop logarithmic terms for SUSY breaking parameters. In the numerical calculation in Sec. IV, however, we use the full renormalization group equation (RGE) and solve it numerically. In Sec. III B, we give a brief description of the SUSY contribution to the muon anomalous magnetic moment and various FCNC and LFV processes.

A. Minimal SUGRA and radiative corrections to the SUSY breaking parameters

The soft SUSY breaking terms of the MSSM are given by

$$\begin{aligned}\mathcal{L}_{\rm soft}=&-(m_Q^2)^i{}_j\tilde{Q}_i^\dagger\tilde{Q}^j-(m_U^2)_i{}^j\tilde{U}^{i*}\tilde{U}_j-(m_D^2)_i{}^j\tilde{D}^{i*}\tilde{D}_j\\&-(m_L^2)^i{}_j\tilde{L}_i^\dagger\tilde{L}^j-(m_E^2)_i{}^j\tilde{E}^{i*}\tilde{E}_j-m_{H_2}^2H_2^\dagger H_2-m_{H_1}^2H_1^\dagger H_1\\&-\{(\tilde{y}_u)_{ij}\tilde{U}^{i*}\tilde{Q}^jH_2+(\tilde{y}_d)_{ij}\tilde{D}^{i*}\tilde{Q}^jH_1+(\tilde{y}_e)_{ij}\tilde{E}^{i*}\tilde{L}^jH_1\\&+\mu BH_1H_2+\text{H.c.}\}-\frac{1}{2}M_1\overline{\tilde{B}}\tilde{B}-\frac{1}{2}M_2\overline{\tilde{W}}\tilde{W}\\&-\frac{1}{2}M_3\overline{\tilde{G}}\tilde{G},\end{aligned}\tag{17}$$

where $\tilde{Q}^i$, $\tilde{U}^{i*}$, $\tilde{D}^{i*}$, $\tilde{L}^i$, and $\tilde{E}^{i*}$ are scalar components of Q^i, $\overline{U}^i$, $\overline{D}^i$, L^i, and $\overline{E}^i$, respectively. We use the same symbols as superfields for scalar components of the Higgs supermultiplets. $\tilde{B}$, $\tilde{W}$, and $\tilde{G}$ are U(1), SU(2), and SU(3) gauginos, respectively. At the GUT scale, these soft SUSY breaking parameters are determined by the following SUSY breaking terms of the SU(5)RN SUSY GUT:

$$\begin{aligned}\mathcal{L}=&-(m_T^2)^i{}_j(\tilde{T}_i^*)_{ab}(\tilde{T}^j)^{ab}-(m_{\overline{F}}^2)^i{}_j(\tilde{\overline{F}}_i^*)^a(\tilde{\overline{F}}^j)_a-(m_{\overline{N}}^2)^i{}_j\tilde{\overline{N}}_i^*\tilde{\overline{N}}^j-(m_H^2)H^*{}_aH^a-(m_{\overline{H}}^2)\overline{H}^{*a}\overline{H}_a\\&-\left\{\frac{1}{8}\epsilon_{abcde}(\tilde{\lambda}_u)_{ij}(\tilde{T}^i)^{ab}(\tilde{T}^j)^{cd}H^e+(\tilde{\lambda}_d)_{ij}(\tilde{\overline{F}}^i)_a(\tilde{T}^j)^{ab}\overline{H}_b+(\tilde{\lambda}_\nu)_{ij}\tilde{\overline{N}}^i(\tilde{\overline{F}}^j)_aH^a+\frac{1}{2}(\tilde{M}_\nu)_{ij}\tilde{\overline{N}}^i\tilde{\overline{N}}^j+\text{H.c.}\right\}\\&-\frac{1}{M_X}\left[\frac{1}{4}\epsilon_{abcde}(\tilde{\kappa}_u^+)_{ij}\{\Sigma^a{}_f(\tilde{T}^i)^{fb}(\tilde{T}^j)^{cd}+(\tilde{T}^i)^{ab}\Sigma^c{}_f(\tilde{T}^j)^{fd}\}H^e+\frac{1}{4}\epsilon_{abcde}(\tilde{\kappa}_u^-)_{ij}\{\Sigma^a{}_f(\tilde{T}^i)^{fb}(\tilde{T}^j)^{cd}\right.\\&\left.-(\tilde{T}^i)^{ab}\Sigma^c{}_f(\tilde{T}^j)^{fd}\}H^e+(\tilde{\kappa}_d)_{ij}(\tilde{\overline{F}}^i)_a\Sigma^a{}_b(\tilde{T}^j)^{bc}\overline{H}_c+(\tilde{\overline{\kappa}}_d)_{ij}(\tilde{\overline{F}}^i)_a(\tilde{T}^j)^b\Sigma^c{}_b\overline{H}_c+(\tilde{\kappa}_\nu)_{ij}\tilde{\overline{N}}^i(\tilde{\overline{F}}^j)_a\Sigma^a{}_bH^b+\text{H.c.}\right]\\&-\frac{1}{2}M_5\overline{\tilde{G}_5}\tilde{G}_5,\end{aligned}\tag{18}$$

where $\tilde{T}^i$, $\tilde{\overline{F}}^i$, and $\tilde{\overline{N}}^i$ are scalar components of T^i, $\overline{F}^i$, and $\overline{N}^i$ and $\tilde{G}_5$ represents the SU(5) gaugino. We assume the minimal supergravity scenario for the origin of SUSY breaking and set the following boundary conditions for the SUSY breaking parameters at the Planck scale:

$$(m_T^2)^i{}_j=(m_{\overline{F}}^2)^i{}_j=(m_{\overline{N}}^2)^i{}_j=m_0^2\delta_j^i,\tag{19a}$$

$$(\tilde{\lambda})_{ij}=m_0A_0(\lambda)_{ij}\qquad(\lambda=\lambda_u,\lambda_d,\lambda_\nu),\tag{19b}$$

$$(\tilde{\kappa})_{ij}=m_0(A_0+\Delta A_0)(\kappa)_{ij}\qquad(\kappa=\kappa_u^\pm,\kappa_d,\overline{\kappa_d},\kappa_\nu),\tag{19c}$$

$$M_5=M_0.\tag{19d}$$

If we ignore radiative corrections from the gauge and Yukawa coupling constants and assume $\Delta A_0=0$, the soft SUSY breaking terms are given by

$$(m_Q^2)^i{}_j=(m_L^2)^i{}_j=(m_U^2)_i{}^j=(m_E^2)_i{}^j=(m_D^2)_i{}^j=m_0^2\delta_i^j,\tag{20a}$$

$$(\tilde{y})_{ij}=m_0A_0(y)_{ij}\qquad(y=y_u,y_d,y_e).\tag{20b}$$

Then LFV processes are forbidden and SUSY contributions to FCNC processes are suppressed. We consider the $\Delta A_0\neq0$ case later.

Radiative corrections between the Planck scale and the EW scale modify the above structure of the soft SUSY breaking terms. In particular, the corrections from the Yukawa coupling constants associated with the colored Higgs supermultiplets and right-handed neutrino supermultiplets are important because they have a different flavor structure from the Yukawa coupling constants of the MSSM.

Let us estimate these corrections using approximate formulas considering only logarithmic terms to see the qualitative features of FCNC/LFV processes in the model. The Yukawa couplings including colored Higgs supermultiplets are parametrized as follows:

$$\begin{aligned}\mathcal{W}_C=&-(y_{CR})_{ij}H_C\overline{U}^i\overline{E}^j-\frac{1}{2}(y_{CL})_{ij}H_CQ^iQ^j\\&-(y_{\overline{C}R})_{ij}\overline{H}_C\overline{D}^i\overline{U}^j-(y_{\overline{C}L})_{ij}\overline{H}_CL^iQ^j+(y_{CN})_{ij}H_C\overline{N}^i\overline{D}^j.\end{aligned}\tag{21}$$

It is convenient to work in the basis where the down-type quark and charged lepton mass matrices are diagonal,

$$(y_u)_{ij}=y_{ui}(V_{\rm CKM})^i{}_j,\tag{22a}$$

$$(y_d)_{ij}=y_{di}\delta_j^i,\tag{22b}$$

$$(y_e)_{ij}=y_{ei}\delta_j^i,\tag{22c}$$

$$(y_\nu)_{ij}=y_{\nu i}(V_L)^i{}_j.\tag{22d}$$

In this basis, Yukawa coupling matrices in Eq. (21) are given by

$$(y_{CR})_{ij}=y_{ui}(V_{\rm CKM}V_E)^i{}_j,\tag{23a}$$

$$(y_{CL})_{ij}=\frac{1}{2}\{(V_{\rm CKM}^T)_i{}^j e^{i\phi_{Uj}} y_{uj}+e^{i\phi_{Ui}} y_{ui}(V_{\rm CKM})^i{}_j\}, \tag{23b}$$

$$(y_{\overline{C}R})_{ij}=y_{di}e^{i\phi_{Ui}}\delta^i_j, \tag{23c}$$

$$(y_{\overline{C}L})_{ij}=y_{ei}(V_E^\dagger)^i{}_j, \tag{23d}$$

$$(y_{CN})_{ij}=y_{\nu i}(V_L V_D)^i{}_j. \tag{23e}$$

The radiative corrections to squark and slepton mass matrices from these Yukawa coupling constants are approximated as follows:

$$\Delta m_Q^2\approx -2(y_u^\dagger y_u+2y_{CL}^\dagger y_{CL}+y_d^\dagger y_d+y_{\overline{C}L}^\dagger y_{\overline{C}L})(3+|A_0|^2) \times m_0^2 t_G-2(y_u^\dagger y_u+y_d^\dagger y_d)(3+|A_0|^2)m_0^2 t_W, \tag{24a}$$

$$\Delta m_U^2\approx -2(2y_u y_u^\dagger+y_{CR}y_{CR}^\dagger+2y_{\overline{C}R}^T y_{\overline{C}R}^*)(3+|A_0|^2)m_0^2 t_G -4y_u y_u^\dagger(3+|A_0|^2)m_0^2 t_W, \tag{24b}$$

$$\Delta m_E^2\approx -2(2y_e y_e^\dagger+3y_{CR}^T y_{CR}^*)(3+|A_0|^2)m_0^2 t_G -4y_e y_e^\dagger(3+|A_0|^2)m_0^2 t_W, \tag{24c}$$

$$\Delta m_D^2\approx -2(2y_d y_d^\dagger+2y_{\overline{C}R}y_{\overline{C}R}^\dagger+y_{CN}^T y_{CN}^*)(3+|A_0|^2) \times m_0^2 t_G-4y_d y_d^\dagger(3+|A_0|^2)m_0^2 t_W, \tag{24d}$$

$$\Delta m_L^2\approx -2(y_e^\dagger y_e+3y_{\overline{C}L}^* y_{\overline{C}L}^T+y_\nu^\dagger y_\nu)(3+|A_0|^2)m_0^2 t_G -2y_e^\dagger y_e(3+|A_0|^2)m_0^2 t_W-2y_\nu^\dagger y_\nu(3+|A_0|^2)m_0^2 t_R, \tag{24e}$$

where we only take account of logarithmic terms so that $t_G=[1/(4\pi)^2]\ln(M_P/M_G)$, $t_R=[1/(4\pi)^2]\ln(M_G/M_R)$, and $t_W=[1/(4\pi)^2]\ln(M_G/M_{\rm SUSY})$. $M_{\rm SUSY}$ is the characteristic mass scale of the SUSY particles and identified with the EW scale. The off-diagonal elements of the above formulas are sources of the LFV and FCNC processes. Keeping only possible large Yukawa coupling constants, the off-diagonal elements of the mass matrices are approximated as follows:

$$(m_Q^2)^i{}_j\approx -2(V_{\rm CKM}^\dagger)^i{}_3 y_t{}^2(V_{\rm CKM})^3{}_j(3+|A_0|^2)m_0^2(t_G+t_W) -\{(V_{\rm CKM}^\dagger)_3{}y_t{}^2\delta^3{}_j+\delta^i{}_3 y_t{}^2(V_{\rm CKM})^3{}_j +(V_{\rm CKM}^\dagger)^i{}_3 y_t{}^2(V_{\rm CKM})^3{}_j(3+|A_0|^2)m_0^2 t_G \quad (i\neq j), \tag{25a}$$

$$(m_E^2)_i{}^j\approx -6(V_E^T V_{\rm CKM}^T)_i{}^3 y_t{}^2(V_{\rm CKM}^* V_E^*)_3{}^j(3+|A_0|^2) \times m_0^2 t_G \qquad (i\neq j), \tag{25b}$$

$$(m_D^2)_i{}^j\approx -2(V_D^T V_L^T)_i{}^k y_{\nu k}{}^2(V_L^* V_D^*)_k{}^j(3 +|A_0|^2)m_0^2 t_G \qquad (i\neq j), \tag{25c}$$

$$(m_L^2)^i{}_j\approx -2(V_L^\dagger)^i{}_k y_{\nu k}{}^2(V_L)^k{}_j(3+|A_0|^2)m_0^2(t_G+t_R) \qquad (i\neq j). \tag{25d}$$

$(m_Q^2)^i{}_j$ corresponds to the flavor mixing due to the large top Yukawa coupling constant which already exists within the MSSM based on the minimal SUGRA. $(m_E^2)_i{}^j$ receives radiative correction from the up-type Yukawa coupling constant between the Planck scale and the GUT scale. This is a well-known mechanism to induce LFV processes in the SUSY GUT [4]. We note the following important features.

There are flavor mixings in the right-handed down-type squark and the left-handed slepton sectors. These mixings are absent in the minimal SUGRA model without right-handed neutrino supermultiplets.

Because V_L can be related to the MNS matrix, large mixing is possible.

The main effect of the higher dimensional operator under the assumption of Eq. (13) is only to rotate the basis of light fermions between d_R and s_R, e_R and μ_R. For each of these mixings the rotation is described by one parameter θ_D in V_D or θ_E in V_E.

In the above discussion, we considered only the radiative correction to squarks and slepton mass matrices; however, the trilinear scalar coupling constants $\tilde{y}_u$, $\tilde{y}_d$, and $\tilde{y}_e$ also receive corrections as follows:

$$(\tilde{y}_u)_{ij}\approx m_0 A_u y_{ui}(V_{\rm CKM})^i{}_j-\frac{m_0 A_0}{3+|A_0|^2} \times\frac{(\Delta m_U^2)_i{}^k y_{uk}(V_{\rm CKM})^k{}_j+y_{ui}(V_{\rm CKM})^i{}_k(\Delta m_Q^2)^k{}_j}{m_0^2}, \tag{26a}$$

$$(\tilde{y}_d)_{ij}\approx m_0 A_d y_{di}\delta^i_j-\frac{m_0 A_0}{3+|A_0|^2}\frac{(\Delta m_D^2)_i{}^j y_{dj}+y_{di}(\Delta m_Q^2)^i{}_j}{m_0^2} -\frac{2}{5}m_0\Delta A\{y_{di}\delta^i_j-(V_D^T)_i{}^k y_{ek}(V_E^\dagger)^k{}_j\}, \tag{26b}$$

$$(\tilde{y}_e)_{ij}\approx m_0 A_e y_{ei}\delta^i_j-\frac{m_0 A_0}{3+|A_0|^2}\frac{(\Delta m_E^2)_i{}^j y_{ej}+y_{ei}(\Delta m_L^2)^i{}_j}{m_0^2} -\frac{3}{5}m_0\Delta A\{y_{ei}\delta^i_j-(V_E^T)_i{}^k y_{dk}(V_D^\dagger)^k{}_j\}, \tag{26c}$$

where A_u, A_d, A_e, and ΔA are given by

$$A_u\approx A_0-\frac{192}{5}g_5^2\frac{M_0}{m_0}t_G-\frac{276}{15}g_5^2\frac{M_0}{m_0}t_W+3y_t^2(t_G+t_W) +\sum_{i=1}^{3}y_{\nu i}{}^2(t_G+t_R), \tag{27a}$$

$$A_d\approx A_0-\frac{168}{5}g_5^2\frac{M_0}{m_0}t_G-\frac{88}{5}g_5^2\frac{M_0}{m_0}t_W, \tag{27b}$$

$$A_e \approx A_0 - \frac{168}{5} g_5^2 \frac{M_0}{m_0} t_G - \frac{48}{5} g_5^2 \frac{M_0}{m_0} t_W, \tag{27c}$$

$$\Delta A \approx -20 g_5^2 \frac{M_0}{m_0} t_G. \tag{27d}$$

The second terms in the right-hand side of Eqs. (26) are induced by the radiative corrections from the Yukawa interactions. The third terms in Eqs. (26b) and (26c) come from the higher dimensional operators. They break proportionality between the trilinear scalar coupling matrix and the corresponding Yukawa coupling matrix and generate flavor mixings in the left-right mixing mass matrices of squarks and sleptons after the EW symmetry breaking. If $\Delta A_0 \neq 0$ in Eq. (19c), we have an extra contribution ΔA_0 to Eq. (27d) and there are corrections of order $m_0^2 A_0 \Delta A_0 \xi t_G$ to Eqs. (25) and corrections of order $m_0 \Delta A_0 \xi t_X$ $(X = G, R, W)$ to Eqs. (26). Notice that even if we assume $\Delta A_0 = 0$ at the Planck scale ΔA is induced by the gauge interaction as shown in Eq. (27d) because the renormalizations of $\tilde{\lambda}_d$ and $\tilde{\kappa}_d$ are different due to the wave-function renormalization of Σ. We therefore expect an analysis with $\Delta A_0 = 0$ to give us qualitative features for the general case.

B. The muon anomalous magnetic moment and FCNC and LFV processes

Let us discuss the muon anomalous magnetic moment and FCNC and LFV processes in the model according to the approximations of the previous section. In the following we make a simplification in the neutrino sector to estimate possible deviations from the SM in the FCNC/LFV processes. We assume the Majorana masses of the right-handed neutrinos are universal at the Majorana mass scale M_R as $(M_\nu)_{ij} = \delta_{ij} M_R$. We also neglect any CP violating phase in the model except for the Kobayashi-Maskawa phase and assume that V_N, V_L, O_ν, and $V_{\rm MNS}$ are real matrices, $\alpha_{D,E} = \beta_{D,E} = \gamma_{D,E} = \delta = 0$ in Eq. (13), and $\phi_{Ui} = 0$ in Eq. (23). If we include these phases, new contributions to the electron and neutron electric dipole moments (EDMs) are induced so that we have to take into account constraints to SUSY parameters from the upper bound of the EDMs. In the numerical calculation we evaluate these EDMs and check that these constraints are satisfied in the case that new CP phases are set to vanish. With the above simplification, the mixing matrix V_L and the neutrino Yukawa coupling can be related to the low energy observables according to Eq. (16),

$$V_L = V_{\rm MNS}^\dagger, \qquad y_{\nu i} = \sqrt{M_R m_{\nu i}} / \langle H_2 \rangle. \tag{28}$$

We parametrize the MNS matrix assuming maximal mixing for the atmospheric neutrino oscillation as follows:

$$V_{\rm MNS} = \begin{pmatrix} \cos\theta_{\rm sun} & \sin\theta_{\rm sun} & 0 \\ -\frac{\sin\theta_{\rm sun}}{\sqrt{2}} & \frac{\cos\theta_{\rm sun}}{\sqrt{2}} & \frac{1}{\sqrt{2}} \\ \frac{\sin\theta_{\rm sun}}{\sqrt{2}} & -\frac{\cos\theta_{\rm sun}}{\sqrt{2}} & \frac{1}{\sqrt{2}} \end{pmatrix}, \tag{29}$$

where $\theta_{\rm sun}$ is the mixing angle for the solar neutrino oscillation. We assume the 1-3 element of the MNS matrix is zero in our analysis because it is known to be small from the result of the CHOOZ experiment [23]. We will comment on the nonzero case later. We assume a hierarchical pattern of neutrino mass, namely, $m_{\nu 1} < m_{\nu 2} \ll m_{\nu 3}$. From the relation

$$m_{\nu 2}^2 = \Delta m_{\rm sun}^2 + m_{\nu 1}^2, \qquad m_{\nu 3}^2 = \Delta m_{\rm atm}^2 + m_{\nu 2}^2, \tag{30}$$

where $\Delta m_{\rm sun}^2$ and $\Delta m_{\rm atm}^2$ are the mass differences of solar and atmospheric neutrino oscillation, $m_{\nu 3}$ and $m_{\nu 2}$ are determined once we fix $m_{\nu 1}$. Then using Eq. (28) we can calculate $y_{\nu i}$ for a fixed value of M_R.

1. The muon anomalous magnetic moment

We consider the SUSY contribution to the muon anomalous magnetic moment [8,21,24,25]. The muon anomalous magnetic moment a_μ is defined by the following effective Lagrangian:

$$\mathcal{L}^{g-2} = \frac{1}{2} \left(\frac{e}{2 m_\mu} \right) a_\mu \bar{\mu} \sigma^{\alpha\beta} \mu F_{\alpha\beta}, \tag{31}$$

where e is the positron charge, m_μ is the muon mass, $F_{\alpha\beta}$ is the electromagnetic field tensor, and $\sigma_{\alpha\beta} = i[\gamma_\alpha, \gamma_\beta]/2$. The SUSY contribution to $a_\mu (\equiv a_\mu^{\rm SUSY})$ is obtained from the flavor diagonal parts of photon-penguin diagrams including smuon-neutralino and sneutrino-chargino. $a_\mu^{\rm SUSY}$ depends on the slepton mass and the neutralino/chargino mass and mixing, but it is rather insensitive to the flavor mixing of the slepton sector. Therefore we expect $a_\mu^{\rm SUSY}$ is almost the same as the result in the minimal SUGRA model. In the MSSM based on the minimal SUGRA, it is known that the main contribution comes from the sneutrino-chargino diagram which contains a component proportional to $\mu \tan\beta$ [25]. Then the $a_\mu^{\rm SUSY}$ preferred by the recent results from the BNL E821 experiment is achieved in the large $\tan\beta$ region of parameter space. In this region the sign of $a_\mu^{\rm SUSY}$ is correlated to the branching ratio of $b \to s\gamma$ through the sign of the Higgsino mass parameter μ so that $a_\mu^{\rm SUSY}$ is positive when $b \to s\gamma$ is suppressed and negative when $b \to s\gamma$ is enhanced.

2. $\mu \to e\,\gamma$, $\tau \to \mu\,\gamma$

We consider LFV decays of charged leptons. Radiative decays of charged leptons occur through photon-penguin diagrams including sleptons, neutralinos, and charginos. The effective Lagrangian for these processes is described as follows:

$$\mathcal{L}^{\rm LFV} = -\frac{4 G_F}{\sqrt{2}} \{ m_{ei} A_R^{ij} (\overline{l_{Ri}} \sigma^{\mu\nu} l_{Lj}) F_{\mu\nu} + m_{ei} A_L^{ij} (\overline{l_{Li}} \sigma^{\mu\nu} l_{Rj}) F_{\mu\nu} \} + \text{H.c.} \qquad (i > j), \tag{32}$$

where G_F is the Fermi constant and i, j denote generation indices. A_R^{ij} corresponds to the amplitude for $l_i^+ \to l_j^+ \gamma_R$ and

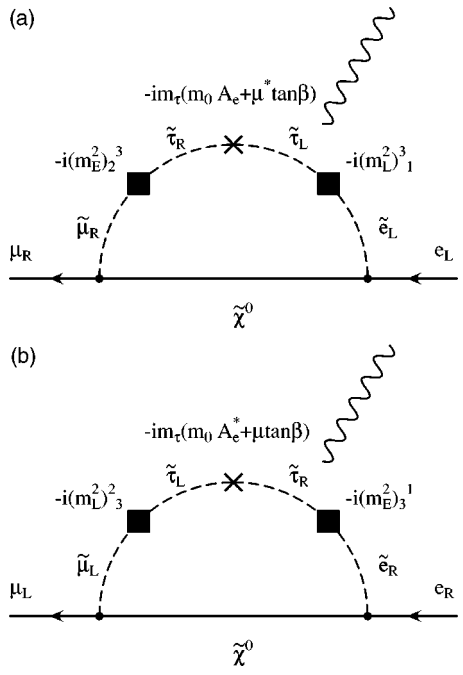

FIG. 1. Possible large contributions to $\mu \to e\gamma$ amplitudes A_R^{21} and A_L^{21} in the present model. They are enhanced by a factor m_τ/m_μ compared to the other contributions.

A_L^{ij} for $l_i^+ \to l_j^+ \gamma_L$. The branching ratios are calculated from these amplitudes as $B(l_i^+ \to l_j^+ \gamma) = 384\pi^2(|A_R^{ij}|^2 + |A_L^{ij}|^2)$.

For $\mu \to e\gamma$, it is known that if both left-handed and right-handed sectors have flavor mixing, there are diagrams that have an enhancement factor m_τ as shown in Fig. 1 [10,16,17]. In our model we find that diagrams corresponding to Figs. 2 and 3 also give large contributions. The flavor mixing in the left-right mixing term in Fig. 3 is induced by renormalization between the Planck and GUT scales as shown in Eq. (26c). Approximate formulas for A_R^{21} and A_L^{21} from these contributions are given by

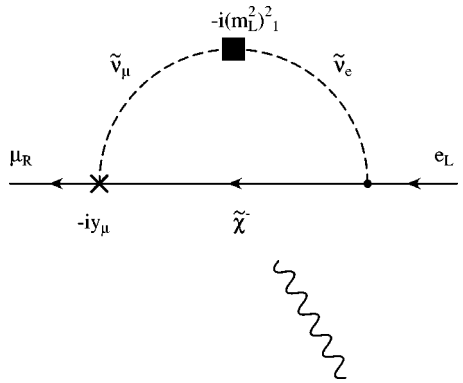

FIG. 2. A possible large contribution to $\mu \to e\gamma$ amplitude A_R^{21} in the present model.

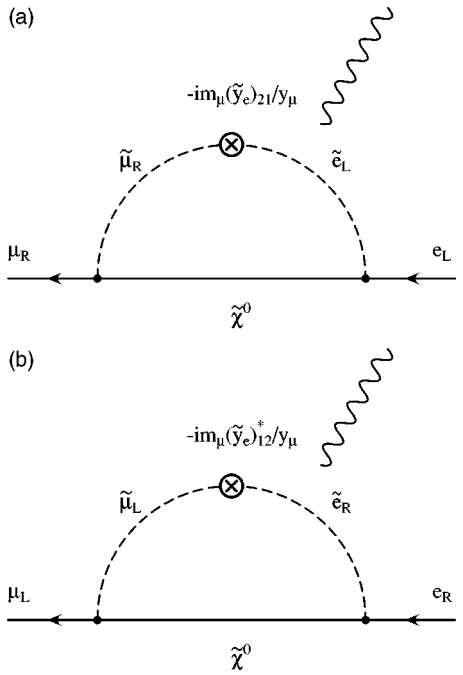

FIG. 3. Possible large contributions to $\mu \to e\gamma$ amplitudes A_R^{21} and A_L^{21} in the present model. The flavor mixing in the left-right mixing is induced by the gauge interaction between the Planck scale and the GUT scale through the wave-function renormalization of **24** Higgs supermultiplet.

$$A_R^{21} \approx \frac{1}{\sqrt{2}} \sin 2\theta_{\rm sun} (y_{\nu 2}{}^2 - y_{\nu 1}{}^2) y_t^2 \times \left[\{ (V_{\rm CKM})^3{}_1 \sin\theta_E + (V_{\rm CKM})^3{}_2 \cos\theta_E \} \frac{m_\tau}{m_\mu} a_2^n - a^c \right] - \cos\theta_E \sin\theta_D a_1^n, \tag{33a}$$

$$A_L^{21} \approx -(y_{\nu 3}{}^2 - y_{\nu 2}{}^2) y_t^2 \{ (V_{\rm CKM})^3{}_1 \cos\theta_E - (V_{\rm CKM})^3{}_2 \sin\theta_E \} \times \frac{m_\tau}{m_\mu} a_2^n + \sin\theta_E \cos\theta_D \, a_1^n, \tag{33b}$$

where we explicitly show the $\theta_{\rm sun}$, $y_{\nu i}$, y_t, θ_E, and θ_D dependence. a_2^n, a^c, and a_1^n are functions of the slepton masses and the chargino and neutralino masses and mixings. These contributions correspond to Fig. 1, Fig. 2, and Fig. 3, respectively. The explicit forms of the functions are given in Appendix B. Because $(V_{\rm CKM})^3{}_2 \gg (V_{\rm CKM})^3{}_1$, the mixing angle θ_E can enhance the amplitude A_L^{21} compared to the case $\theta_E = 0$.

The ratio of the magnitudes of A_L^{21} and A_R^{21} can be measured by the P-odd asymmetry of the $\mu \to e\gamma$ process, $A(\mu \to e\gamma)$ [26]. With the help of initial muon polarization, we define $A(\mu \to e\gamma)$ as follows:

$$\frac{dB(\mu^+ \to e^+\gamma)}{d\cos\theta} = \frac{1}{2} B(\mu^+ \to e^+\gamma) \{ 1 + A(\mu^+ \to e^+\gamma) \times P \cos\theta \}, \tag{34a}$$

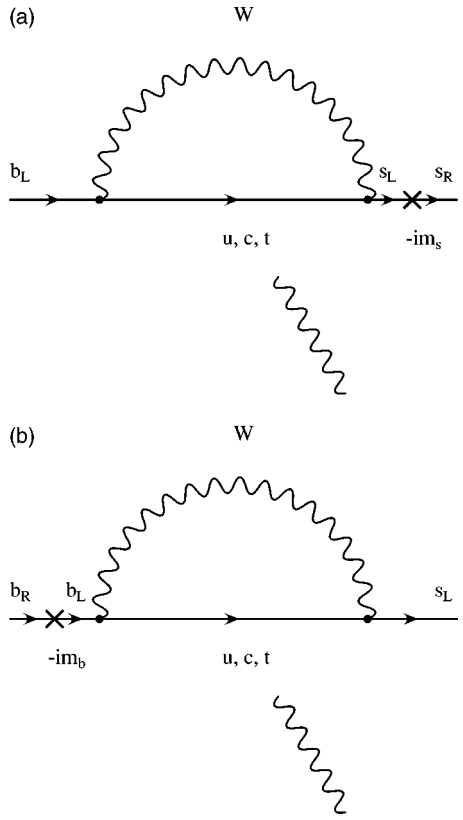

FIG. 4. One-loop diagrams that contribute to $b\to s\gamma$ in the SM. The contribution to C_7' (a) is suppressed by m_s/m_b compared to the contribution to C_7 (b).

$$A(\mu^+\to e^+\gamma)=\frac{|A_L^{21}|^2-|A_R^{21}|^2}{|A_L^{21}|^2+|A_R^{21}|^2}, \tag{34b}$$

where P is the polarization of the initial μ^+ and θ is the angle between the polarization and the momentum of the decay positron. For $\tau\to\mu\gamma$, a similar P-odd asymmetry can be measured in the $e^+e^-\to\tau^+\tau^-$ process using spin correlation of the τ pair [27].

3. $b\to s\gamma$

The $\Delta B=1$ FCNC effective Lagrangian for the radiative B decay is written as follows:

$$\mathcal{L}^{\Delta S=1}=-\frac{4G_F}{\sqrt{2}}\{C_7'(\overline{s_R}\sigma^{\mu\nu}b_L)F_{\mu\nu}+C_7(\overline{s_L}\sigma^{\mu\nu}b_R)F_{\mu\nu}\}+\text{H.c.} \tag{35}$$

In the SM case, the process occurs through photon-penguin diagrams which exchange a W boson as in Fig. 4 and C_7' is suppressed by a factor of m_s/m_b compared to C_7. In the minimal SUGRA model without the right-handed neutrino supermultiplets, the flavor mixing in the squark mass matrices appears only in that of the left-handed squark and the same argument can be applied. In the present model, however, a gluino exchanging diagram (Fig. 5) can give a large contribution to C_7' because of the new flavor mixing in the right-handed down-type squarks $(m_D^2)_2{}^3$.

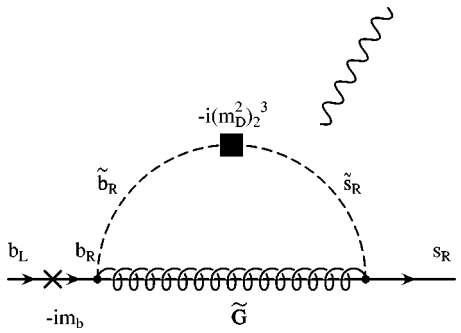

FIG. 5. A possible large contribution to $b\to s\gamma$ amplitude C_7' in the SU(5)RN SUSY GUT that is not suppressed by m_s/m_b.

If C_7' has a similar magnitude to C_7, the time-dependent CP asymmetry of $B\to M_s\gamma$ may be observed where M_s is a CP eigenstate which includes a strange quark such as K_1 $(\to K_S\rho^0)$ or K^* $(\to K_S\pi^0)$ [19,28]. The asymmetry is defined as follows:

$$\frac{\Gamma(t)-\overline{\Gamma}(t)}{\Gamma(t)+\overline{\Gamma}(t)}=\eta A_{CP}(B\to M_s\gamma)\sin\Delta m_{B_d}t,$$

$$A_{CP}(B\to M_s\gamma)=\frac{2\,\mathrm{Im}(e^{-i\theta_B}C_7C_7')}{|C_7|^2+|C_7'|^2}, \tag{36}$$

where $\Gamma(t)$ $[\overline{\Gamma}(t)]$ is the decay width of $B^0(t)\to M_s\gamma$ $[\overline{B}^0(t)\to M_s\gamma]$. η is $+1$ if M_s is a CP even state and -1 if M_s is a CP odd state. θ_B is the phase of the B_d-$\overline{B}_d$ mixing amplitude $M_{12}(B_d)$ which is defined below in Eq. (40). In the SM case, this asymmetry is only a few percent; however, it may be considerably enhanced by the new SUSY contribution to C_7'.

4. ε_K

K^0-$\overline{K}^0$ mixing is described by the $\Delta S=2$ FCNC effective Lagrangian. The general form is given by

$$\begin{aligned}\mathcal{L}^{\Delta S=2}=-\frac{8G_F}{\sqrt{2}}\Big\{&\frac{1}{2}g_R^V(\overline{d}_R^\alpha\gamma^\mu s_{R\alpha})(\overline{d}_R^\beta\gamma_\mu s_{R\beta})\\&+\frac{1}{2}g_L^V(\overline{d}_L^\alpha\gamma^\mu s_{L\alpha})(\overline{d}_L^\beta\gamma_\mu s_{L\beta})+\frac{1}{2}g_{RR}^S(\overline{d}_L^\alpha s_{R\alpha})\\&\times(\overline{d}_L^\beta s_{R\beta})+\frac{1}{2}g_{LL}^S(\overline{d}_R^\alpha s_{L\alpha})(\overline{d}_R^\beta s_{L\beta})\\&+\frac{1}{2}g_{RR}^S{}'(\overline{d}_L^\alpha s_{R\beta})(\overline{d}_L^\beta s_{R\alpha})+\frac{1}{2}g_{LL}^S{}'(\overline{d}_R^\alpha s_{L\beta})(\overline{d}_R^\beta s_{L\alpha})\\&+g_{RL}^S(\overline{d}_L^\alpha s_{R\alpha})(\overline{d}_R^\beta s_{L\beta})+g_{RL}^S{}'(\overline{d}_L^\alpha s_{R\beta})(\overline{d}_R^\beta s_{L\alpha})\Big\}\\&+\text{H.c.},\end{aligned} \tag{37}$$

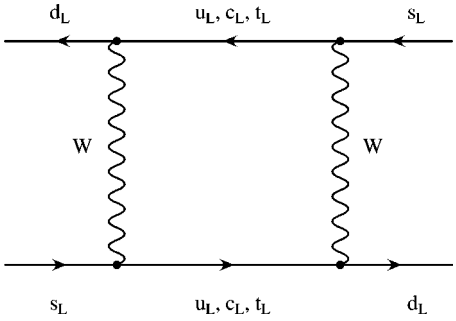

FIG. 6. A one-loop diagram that contributes to ε_K in the SM. A similar diagram that contributes to B_d-$\overline{B}_d$ (B_s-$\overline{B}_s$) mixing in the SM can be obtained by replacing quarks in the external lines so that $s \to b$ ($s \to b$ and $d \to s$).

where α and β denote color indices. The explicit forms of the effective coupling constants in the above formula are given in Appendix C. The CP violation parameter in K^0-$\overline{K}^0$ mixing, ε_K, is calculated from the above formula as follows:

$$\varepsilon_K = \frac{e^{(\pi/4)i}}{\sqrt{2}} \frac{\mathrm{Im}\{M_{12}(K)\}}{\Delta m_K},$$

$$M_{12}(K) = -\frac{\langle K^0 | \mathcal{L}^{\Delta S=2} | \overline{K}^0 \rangle}{2m_K}. \tag{38}$$

In the case of the SM, the process occurs through a box diagram in which two W bosons are exchanged between the down-type quarks (Fig. 6) so that it is dominated by the g_L^V term. However, we have a new flavor mixing $(m_D^2)_1{}^2$ in the right-handed down-type squark sector. We can draw gluino exchanging diagrams like Fig. 7 which include the CP violating phase of the CKM matrix in $(m_Q^2)^1{}_2$ on one of the squark lines and large flavor mixing in $(m_D^2)_1{}^2$ on the other. These diagrams contribute to the coupling constants g_{RL}^S and $g_{RL}^S{}'$. In the actual numerical calculation we first derive the effective Lagrangian at the energy scale M_{SUSY}. According to Ref. [29], we include QCD corrections and derive the

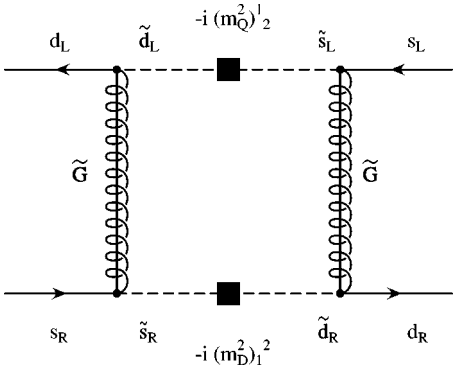

FIG. 7. A possible large contribution to ε_K in the SU(5)RN SUSY GUT. There is also a crossed diagram because of the Majorana nature of the gluino.

effective Lagrangian at the hadronic scale. The matrix elements for the dominant operators are parametrized as follows:

$$\langle K^0 | (\bar{d}_L^\alpha \gamma^\mu s_{L\alpha})(\bar{d}_L^\beta \gamma_\mu s_{L\beta}) | \overline{K}^0 \rangle = \frac{2}{3} m_K^2 f_K^2 B_K, \tag{39a}$$

$$\langle K^0 | (\bar{d}_R^\alpha s_{L\alpha})(\bar{d}_L^\beta s_{R\beta}) | \overline{K}^0 \rangle = \frac{1}{2}\left(\frac{m_K}{m_s + m_d}\right)^2 m_K^2 f_K^2 (B_K)_{RL}^S, \tag{39b}$$

$$\langle K^0 | (\bar{d}_R^\alpha s_{L\beta})(\bar{d}_L^\beta s_{R\alpha}) | \overline{K}^0 \rangle = \frac{1}{6}\left(\frac{m_K}{m_s + m_d}\right)^2 m_K^2 f_K^2 (B_K)_{RL}^S{}', \tag{39c}$$

where B_K, $(B_K)_{RL}^S$, and $(B_K)_{RL}^S{}'$ are bag parameters calculated by the lattice QCD method. Because there is a large enhancement factor of order $(m_K/m_s)^2$ in the matrix elements and large mixings originate from the MNS matrix, the SUSY contribution to ε_K is expected to be large in this model.

5. B_d-$\overline{B}_d$/B_s-$\overline{B}_s$ mixing

The $\Delta B = 2$ effective Lagrangians for B_d-$\overline{B}_d$ and B_s-$\overline{B}_s$ mixing are parametrized in the same manner as K^0-$\overline{K}^0$ mixing. For B_d-$\overline{B}_d$ mixing, it is obtained by replacing the strange quark with the bottom quark in Eq. (37). For B_s-$\overline{B}_s$ mixing, we further replace the down quark by the strange quark. The mass difference of B_d-$\overline{B}_d$ mixing, Δm_{B_d}, is calculated from the effective Lagrangian as follows:

$$\Delta m_{B_d} = 2|M_{12}(B_d)|, \qquad M_{12}(B_d) = -\frac{\langle B_d^0 | \mathcal{L}^{\Delta B=2} | \overline{B}_d^0 \rangle}{2m_{B_d}}. \tag{40}$$

In the SM case, this process occurs through the W boson exchanging diagram and the g_L^V term gives the dominant contribution. In the present case, there are new diagrams as shown in Fig. 8, which contain the new flavor mixing in $(m_D^2)_1{}^3$ on one of the down-type squark lines or on both of them. The former contributes to g_{RL}^S and $g_{RL}^S{}'$ and the latter to g_R^V. Unlike K^0-$\overline{K}^0$ mixing, the scalar-scalar matrix elements do not have an enhancement factor for B_d-$\overline{B}_d$ mixing because m_{B_d}/m_b is $O(1)$. A similar argument holds for B_s-$\overline{B}_s$ mixing. In the numerical calculation we use the next to leading order QCD correction for g_R^V and g_L^V and leading order QCD formulas for other contributions [29] and bag parameters are calculated by lattice QCD. Numerical values are shown later.

IV. RESULTS OF NUMERICAL CALCULATIONS

In this section we present our numerical results for the FCNC/LFV processes in the SU(5)RN SUSY GUT.

In the present analysis we assume that the SUSY breaking terms have the minimal SUGRA-type boundary condition at

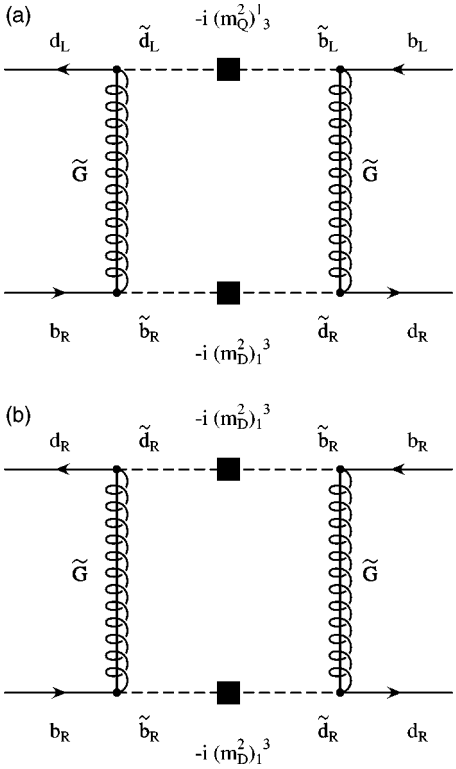

FIG. 8. Possible large contributions to B_d-$\overline{B_d}$ mixing in the present model. Similar diagrams that contribute to B_s-$\overline{B_s}$ mixing can be obtained by replacing the down quark/squark in the diagrams with the strange quark/squark. There are also crossed diagrams.

the Planck scale and that the Kähler potential is flat. Adopting the simplifications discussed in the previous section, we have the following input parameters.

Parameters at the Planck scale: the universal scalar mass m_0, the universal gaugino mass M_0, and the universal coefficient for the scalar couplings A_0.

Parameters at the GUT scale: mixing angles θ_D and θ_E.

A parameter at the right-handed neutrino mass scale: Majorana mass of the right-handed neutrino M_R, which is also used as the matching scale.

Parameters at the EW scale: quark, lepton, and neutrino masses, mixing matrices $V_{\rm CKM}$ and $V_{\rm MNS}$, $\tan\beta$, and the sign of the Higgsino mass parameter μ in Eq. (2).

Throughout the following calculation, we fix some of the parameters as shown in Table I. We consider two cases for the neutrino parameters, corresponding to the large mixing angle (LMA) and the small mixing angle (SMA) MSW solutions of the solar neutrino anomaly. The parameters we used in the neutrino sector for each case are given in Table II. For M_R and $\tan\beta$, we take several cases to see the dependences (see Table III). SUSY breaking parameters m_0, M_0,

TABLE I. Input parameters used in the numerical calculation. $|V_{ub}/V_{cb}|$ and δ_{13} are varied in Fig. 14 below.

$m_t^{\rm pole}$	$m_b^{\rm pole}$	$m_s^{\overline{\rm MS}}$(2 GeV)	V_{cb}	$\lvert V_{ub}/V_{cb}\rvert$	δ_{13}
175 GeV	4.8 GeV	120 MeV	0.04	0.08	60°

TABLE II. Parameters for the neutrino sector. LMA (SMA) corresponds to the large (small) mixing angle MSW solution for the solar neutrino anomaly.

	LMA	SMA
$\sin^2 2\theta_{\rm sun}$	1	5.5×10^{-3}
$\sin^2 2\theta_{\rm atm}$	1	1
θ_{13}	0	0
Δm_{12}^2 (eV^2)	1.8×10^{-5}	5.0×10^{-6}
Δm_{23}^2 (eV^2)	3.5×10^{-3}	3.5×10^{-3}
m_{ν_1} (eV)	4.0×10^{-3}	2.2×10^{-3}

and A_0 are varied and ΔA_0 is fixed to zero.

With these parameters, we solve the RGEs of the mass parameters and the coupling constants between the Planck and the EW scale taking all the flavor mixings into account. Details of our method are explained in Appendix A. The magnitude of μ is determined by the radiative EW symmetry breaking condition, in which the minimum of the one-loop effective potential for the Higgs fields is evaluated. Then we obtain all the masses and mixings of the SUSY particles at the EW scale and calculate the FCNC/LFV observables as functions of the above parameters. We calculate the following quantities: the SUSY contribution to the muon anomalous magnetic moment $a_\mu^{\rm SUSY}$; branching ratios of $b\to s\gamma$, $\mu\to e\gamma$, and $\tau\to\mu\gamma$; P-odd asymmetry of $\mu\to e\gamma$; B^0-$\overline{B^0}$ mass splittings Δm_{B_d} and Δm_{B_s}; CP violation parameter ε_K; and time-dependent CP asymmetries of $B\to M_s\gamma$ and $B\to J/\psi K_S$.

In order to find the allowed region in parameter space, we impose constraints from the experimental results of the direct searches for SUSY particles [30] and Higgs bosons [31] and the measurements of $B(b\to s\gamma)$ [32]. Also it turns out that, in some parameter region, the branching ratio of $\mu\to e\gamma$ exceeds the present upper limit and hence this process already gives an important constraint on the parameter space. We discuss the constraints from the measured values of ε_K and Δm_{B_d} and the lower bound of Δm_{B_s} later, since it depends on the CKM parameters, namely, $|V_{ub}|$ and δ_{13} [33].

A. θ_E and θ_D dependence of $\mu\to e\gamma$ and ε_K

Let us first discuss the θ_E and θ_D dependence of the $\mu\to e\gamma$ decay and ε_K.

As given in Eq. (33), the decay amplitudes A_R^{21} and A_L^{21} depend on θ_E and θ_D differently, so that both the branching ratio and P-odd asymmetry are affected. In Fig. 9 we show $B(\mu\to e\gamma)$ and $A(\mu\to e\gamma)$ as functions of θ_E and θ_D. The shaded regions are excluded by the upper bound of $B(\mu\to e\gamma)$ [34]. Here we take the LMA case for the neutrino parameters, $M_R=4\times10^{13}$ GeV, $\tan\beta=20$, $\mu>0$. SUSY breaking parameters are also fixed as $M_0=300$ GeV, $A_0=0$, and $m_0=0$, 300, 600, 900 GeV. For the fixed $\theta_D=0$ case [(a) and (b)], we can see that the amplitude A_L^{21} is enhanced for a nonvanishing θ_E and relatively small m_0. In the parameter region $\theta_E\sim90°$, $B(\mu\to e\gamma)$becomes larger than that for $\theta_E\sim0$ and $A(\mu\to e\gamma)$ approaches $+1$, reflecting the

TABLE III. Parameters for Fig. 11.

	(a)	(b)	(c)	(d)	(e)	(f)	(g)
neutrino	LMA	LMA	LMA	LMA	LMA	SMA	SMA
M_R (GeV)	4×10^{13}	4×10^{13}	4×10^{13}	4×10^{13}	4×10^{14}	4×10^{13}	4×10^{14}
θ_D	0	0	45°	0	0	0	0
$\tan\beta$	20	20	20	5	20	20	5
A_0	0	2	0	0	0	0	2.5

fact that A_L^{21} is enhanced and dominates A_R^{21}. For the $\theta_E=0$ case [(c) and (d)], A_R^{21} dominates in most of the range of θ_D and hence $A(\mu\to e\gamma)$ is close to -1. In some special case, $\theta_D=-30°$ and $m_0=300$ GeV for example, a cancellation among contributions to A_R^{21} occurs and the branching ratio is suppressed. In such a case the *P*-odd asymmetry approaches $+1$.

Figure 10 shows the θ_D dependence of ε_K for the same parameter set as in Figs. 9(c) and (d). This dependence comes from g_{RL}^S and $g_{RL}^S{}'$ in Eq. (37) since θ_D directly affects the mixing between the right-handed down-type squarks of the first and second generations. We have checked that the θ_E dependence is negligible for ε_K.

Hereafter we fix θ_E as $\theta_E=0$ and in most cases we also fix $\theta_D=0$.

B. $a_\mu^{\rm SUSY}$, FCNC, and LFV observables for different sets of the neutrino and the SUSY parameters

In Fig. 11 we show contour plots of the SUSY contribution to the muon anomalous magnetic moment $a_\mu^{\rm SUSY}$, branching ratios of $\mu\to e\gamma$ and $\tau\to\mu\gamma$, and the deviations from the SM values of ε_K, Δm_{B_d}, and Δm_{B_s}. The input parameters used in each figure are given in Table III. We also fix the sign of μ as $\mu>0$ in these figures. The $\mu<0$ region is disfavored because the SUSY contributions to the $b\to s\gamma$ decay amplitude interfere with the SM contribution constructively, so that the branching ratio becomes too large in a large portion of the parameter space. Note that the constraints from ε_K, Δm_{B_d}, and Δm_{B_s} are not imposed in Fig. 11 since these constraints depend on δ_{13} and $|V_{ub}|$. We show our result for each of these observables by taking the ratio to

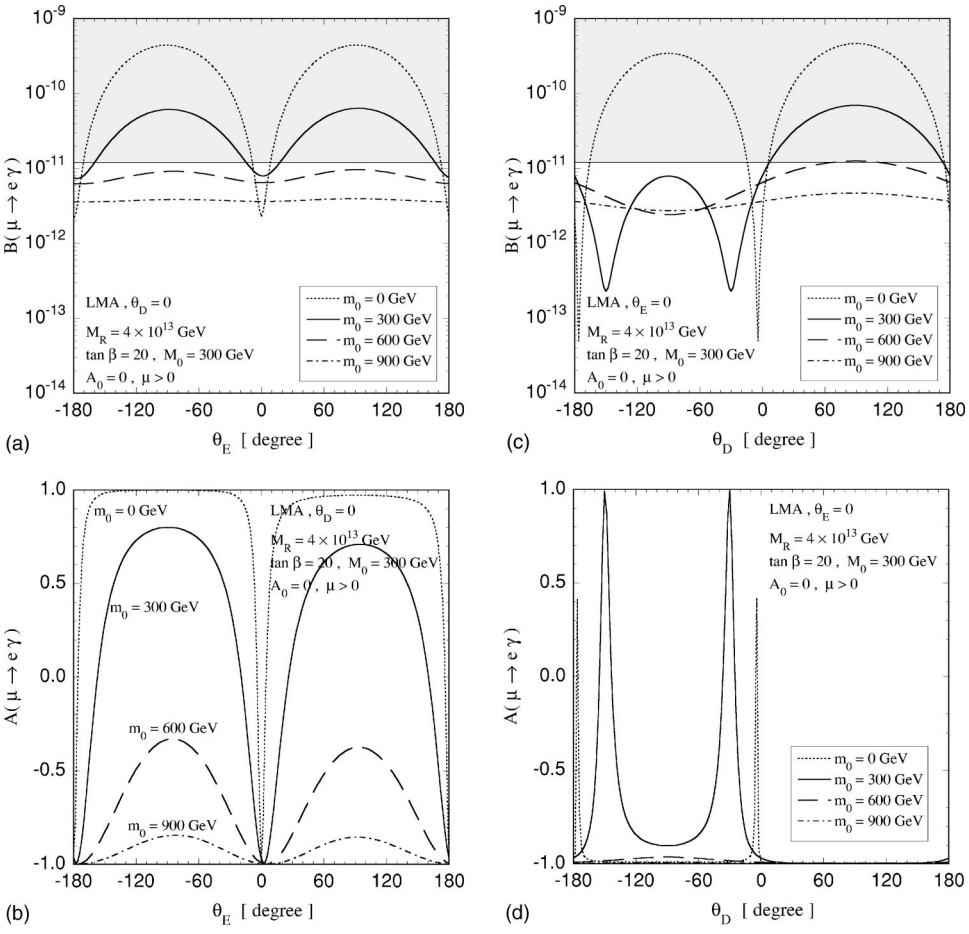

FIG. 9. Branching ratio and *P*-odd asymmetry of $\mu\to e\gamma$ as functions of θ_E and θ_D.

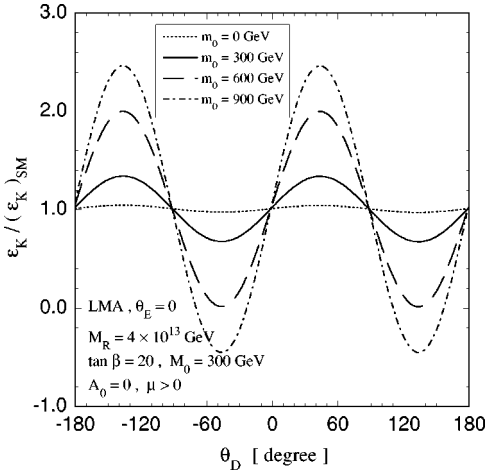

FIG. 10. ε_K normalized to the SM value as a function of θ_D. Parameters are the same as those in Figs. 9(c) and (d).

the corresponding SM value, expecting that most of the dependences on the CKM parameters cancel. In fact we have checked that the plots do not change when a different value of δ_{13} is used. The dependences of $a_\mu^{\rm SUSY}$, $B(\mu\to e\,\gamma)$, and $B(\tau\to\mu\,\gamma)$ on the CKM parameters are also small.

In Fig. 11(a) we take the LMA case for the neutrino masses and mixing, $M_R=4\times10^{13}$ GeV, $\theta_E=\theta_D=0$, $\tan\beta=20$, and $A_0=0$, as a reference point. Shaded regions are experimentally excluded regions. The constraints mainly come from the LEP II Higgs boson search and the upper bound on $B(\mu\to e\,\gamma)$. We see that there is a parameter region with $20\times10^{-10}\lesssim a_\mu^{\rm SUSY}\lesssim60\times10^{-10}$, which is favored by the E821 result and in that region $B(\mu\to e\,\gamma)$ becomes larger than 10^{-12}. In the allowed parameter region within the plotted range $M_0<1$ TeV and $m_0<4$ TeV, $B(\mu\to e\,\gamma)$ varies from $O(10^{-14})$ to $O(10^{-11})$ and $B(\tau\to\mu\,\gamma)$varies from $O(10^{-11})$ to $O(10^{-9})$. Both branching ratios depend similarly on M_0 and m_0. Also we see that the deviation of ε_K from the SM value is about 10% at most and the deviations of Δm_{B_d} and Δm_{B_s} are small.

In Fig. 11(b) plots for $A_0=2$ are given. In this case the stop mass squared becomes negative in some parameter region, which is shown in the figure. The region excluded by the $B(\mu\to e\,\gamma)$ constraint is enlarged, due to the enhancement of the branching ratio by the change in the left-right mixing in the slepton mass matrices. The deviation of ε_K is also enhanced and there is an allowed parameter region where ε_K is enhanced by more than 25%. It is noticeable that

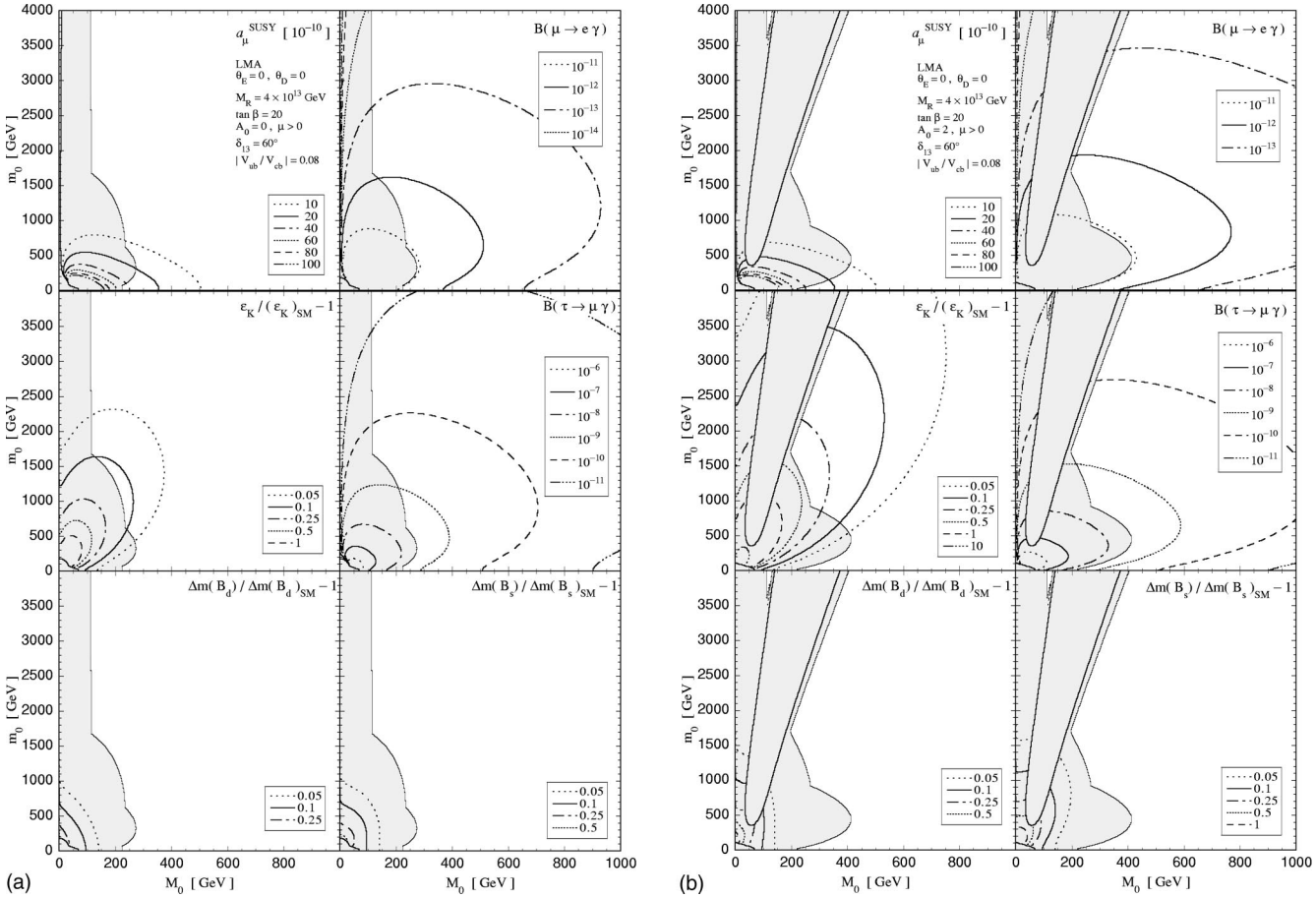

FIG. 11. Contour plots of $a_\mu^{\rm SUSY}$, $B(\mu\to e\,\gamma)$, $B(\tau\to\mu\,\gamma)$, $\varepsilon_K/\varepsilon_K^{\rm SM}-1$, $\Delta m_{B_d}/\Delta m_{B_d}^{\rm SM}-1$, and $\Delta m_{B_s}/\Delta m_{B_s}^{\rm SM}-1$ on the m_0–M_0 plane for various choices of the parameters given in Table III. CKM parameters are fixed as $\delta_{13}=60°$ and $|V_{ub}/V_{cb}|=0.08$ and μ is taken as positive. Shaded regions are excluded experimentally (see text). In (b) and (g), the excluded regions corresponding to negative stop mass squared are also shown.

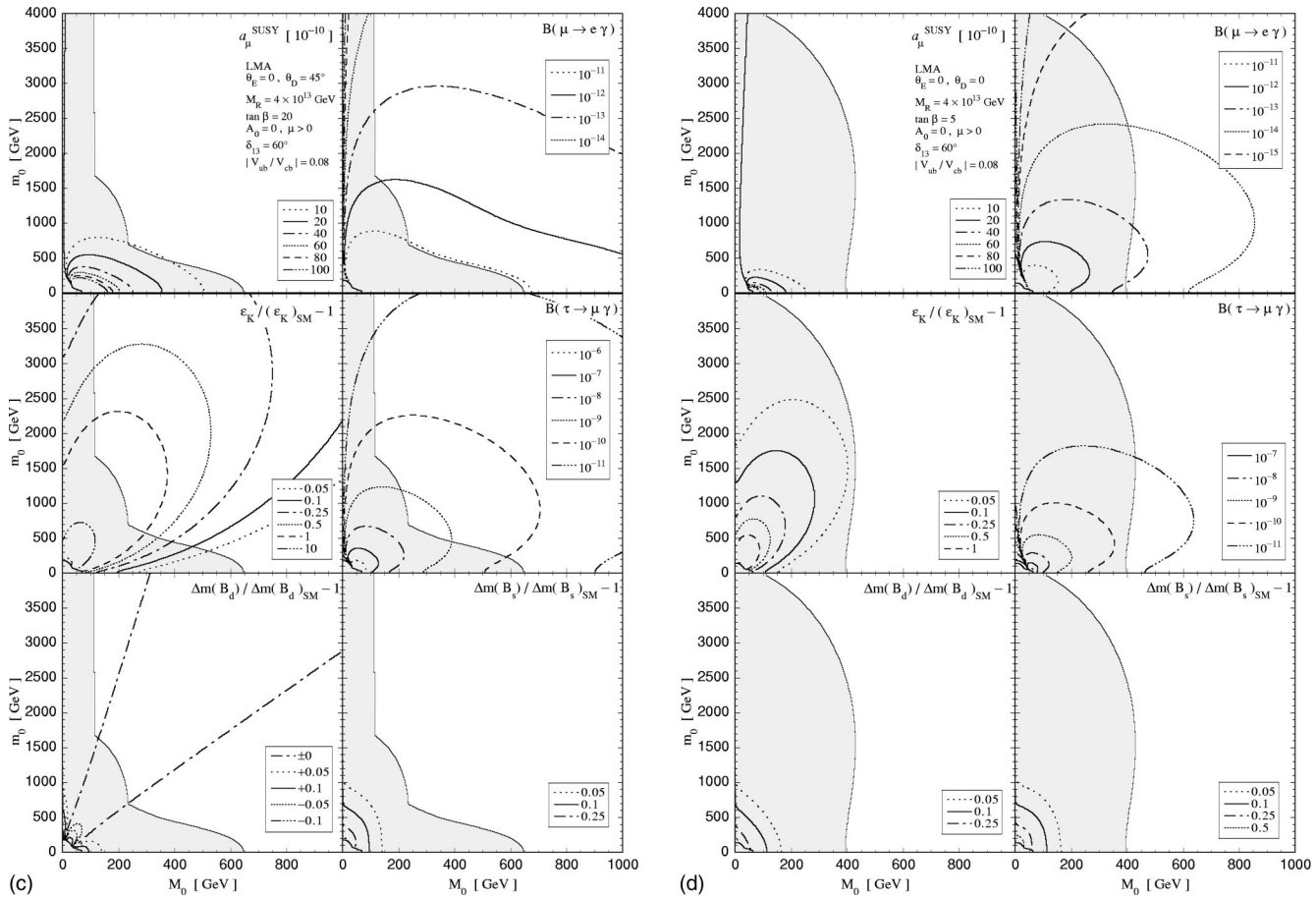

FIG. 11. (*Continued*).

the allowed parameter region with a large enhancement of ε_K is different from the E821-favored region. The region that corresponds to both a favorable $a_\mu^{\rm SUSY}$ and a large enhancement of ε_K is excluded by other constraints, such as $B(\mu \to e\gamma)$.

Comparing Figs. 11(a) and (c), we can see the dependence on θ_D. Since θ_D affects the mixing between the first and the second generations, the difference appears mainly for $B(\mu \to e\gamma)$ and ε_K. For a nonvanishing $\theta_D = 45°$ [Fig. 11(c)], $B(\mu \to e\gamma)$ is enhanced for $m_0 \lesssim 700$ GeV and the excluded region is enlarged. Also the SUSY contribution to ε_K can be larger than the SM contribution in a part of the allowed parameter region as shown in Fig. 10. $a_\mu^{\rm SUSY}$does not depend on θ_D so that the parameter region with $a_\mu^{\rm SUSY} \gtrsim 10 \times 10^{-10}$ is excluded in the case (c). The behavior of $B(\tau \to \mu\ \gamma)$ and Δm_{B_s} is unchanged also. Although Δm_{B_d} depends on θ_D, the deviation is quite small in either case.

The plots for $\tan\beta = 5$ are given in Fig. 11(d). Since both $B(\mu \to e\gamma)$and $B(\tau \to \mu\gamma)$ are proportional to $\tan^2\beta$, possible values are suppressed as $\mathrm{B}(\mu \to e\gamma) \lesssim 10^{-13}$ and $\mathrm{B}(\tau \to \mu\gamma) \lesssim 10^{-10}$. $a_\mu^{\rm SUSY}$ is proportional to $\tan\beta$ and is also suppressed. The excluded region is larger than in the $\tan\beta = 20$ case because the constraint from the Higgs boson mass bound is stronger for a smaller $\tan\beta$. The plots for ε_K, Δm_{B_d}, and Δm_{B_s} are the same as those in the case (a) except that the excluded region is enlarged.

Figure 11(e) shows the case with a larger $M_R = 4 \times 10^{14}$ GeV. Since the magnitude of the neutrino Yukawa coupling constants are proportional to $\sqrt{M_R}$, the flavor mixings in m_D^2 and m_L^2 are enhanced for a larger M_R. As a result we see that $B(\mu \to e\gamma)$, $B(\tau \to \mu\gamma)$, and ε_K are significantly enhanced in this case, compared to the $M_R = 4 \times 10^{13}$ GeV case (a). Although the excluded region due to the constraint from $B(\mu \to e\gamma)$ is enlarged, there is still an allowed parameter region where ε_K is enhanced by more than 50% of the SM value. Also $B(\tau \to \mu\gamma)$ can be close to $O(10^{-8})$. In the allowed parameter region, the deviations of Δm_{B_d} and Δm_{B_s} are small. $a_\mu^{\rm SUSY}$ is unaffected by the change of M_R and the E821-favored region is excluded by the $B(\mu \to e\gamma)$ constraint.

Figure 11(f) shows the SMA case. Other parameters are taken to be the same as those in the case (a). In this case, the mixing between the first and second generations is suppressed compared to the LMA case. Consequently $B(\mu \to e\gamma)$ is at most $O(10^{-13})$ in the allowed region and the deviation of ε_K is smaller. $a_\mu^{\rm SUSY}$, $B(\tau \to \mu\ \gamma)$, Δm_{B_d}, and Δm_{B_s} look the same as those in case (a).

In all the above cases the deviation of the B^0-$\overline{B^0}$ mixing from the SM value is small. Let us now show an example with a large enhancement of the B_s-$\overline{B_s}$ mixing in Fig. 11(g). We see that Δm_{B_s}differs from the SM value by more than

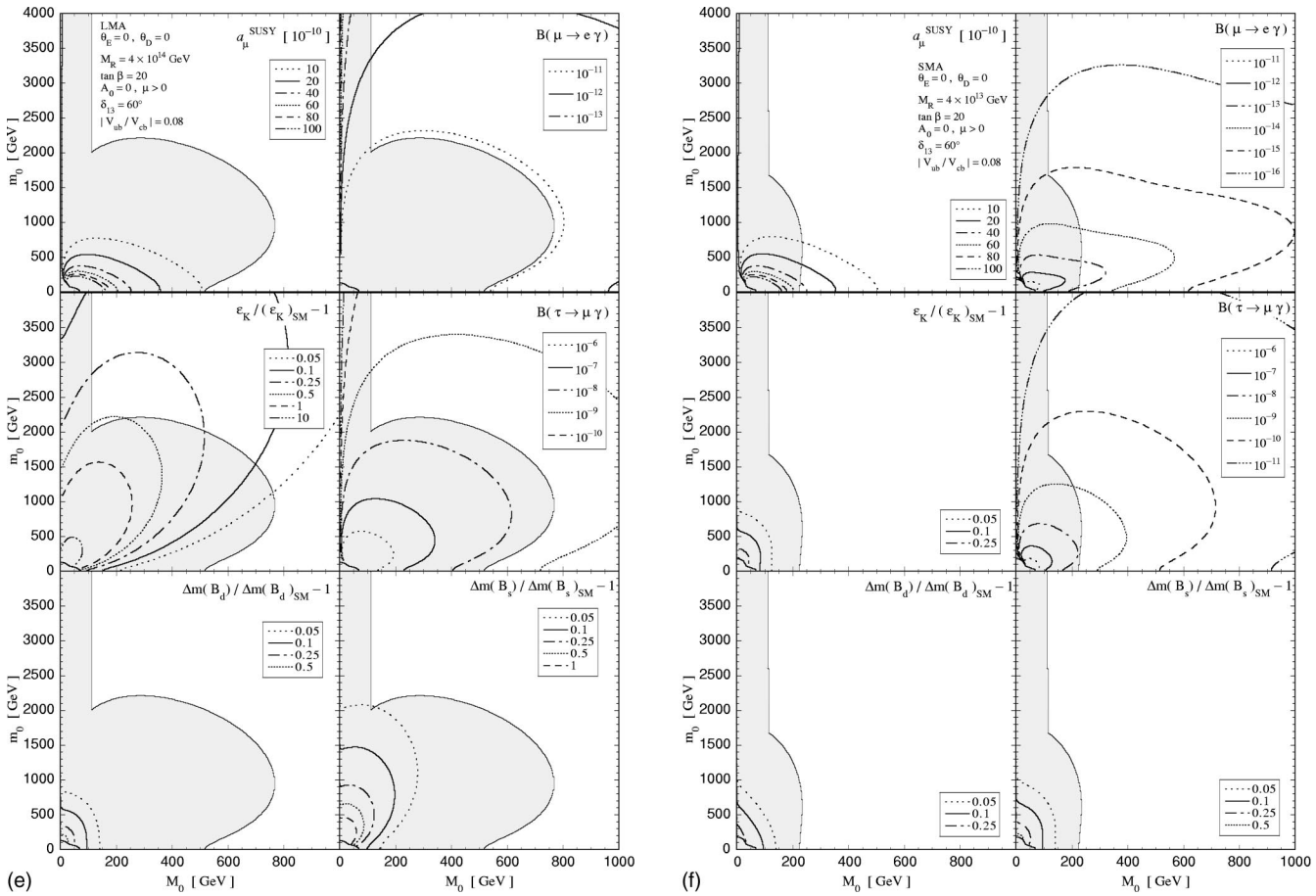

FIG. 11. (*Continued*).

50% in the parameter region $m_0 \gtrsim 700$ GeV and $M_0 \lesssim 200$ GeV. In the same region ε_K is also enhanced by a similar amount. Note that this enhancement comes from mixing in the right-handed down-type squarks induced by the neutrino Yukawa coupling. In such a case the time-dependent CP asymmetry of $B \to M_s \gamma$ decay is also enhanced. Figure 12 shows $A_{CP}(B \to M_s \gamma)$ with the same parameter set. We see that this asymmetry can be larger than 25% in the parameter region where Δm_{B_s} is enhanced. In this case $B(\tau \to \mu\gamma)$can be close to 10^{-7}.

In Table IV we summarize the possible SUSY contributions to the observables given in Fig. 11. We can see that, except for the case (g), a large deviation from the SM is possible only in $a_\mu^{\rm SUSY}$, $B(\mu \to e\gamma)$, and ε_K.

Let us look at the correlation among $a_\mu^{\rm SUSY}$, $B(\mu \to e\gamma)$, and ε_K more closely. Figure 13 shows the correlation between $a_\mu^{\rm SUSY}$and $B(\mu \to e\gamma)$, $a_\mu^{\rm SUSY}$and $\varepsilon_K/(\varepsilon_K)_{\rm SM}$, and $\varepsilon_K/(\varepsilon_K)_{\rm SM}$ and $B(\mu \to e\gamma)$. Here SUSY breaking parameters m_0, M_0, and A_0 are scanned within the range $m_0, M_0 < 3$ TeV, and $-5 < A_0 < 5$. Other parameters are taken to be the same as those in Figs. 11(a) and (b). In the plot of the correlation between $a_\mu^{\rm SUSY}$and $B(\mu \to e\gamma)$, the $a_\mu^{\rm SUSY} < 0$ branch corresponds to $\mu < 0$ and the $a_\mu^{\rm SUSY} \lesssim -20 \times 10^{-10}$ region is excluded by the $B(b \to s\gamma)$ constraint. Notice that the parameter region where $a_\mu^{\rm SUSY}$saturates the E821 result is different from that with a large $\varepsilon_K/(\varepsilon_K)_{\rm SM}$. As can be seen in the plot of $a_\mu^{\rm SUSY}$and $\varepsilon_K/(\varepsilon_K)_{\rm SM}$, when ε_K is enhanced by $\sim 50\%$, the magnitude of $a_\mu^{\rm SUSY}$is small.

C. Allowed region of $\Delta m_{B_s}/\Delta m_{B_d}$ and the CP asymmetry of $B \to J/\psi K_S$

Finally, let us discuss the effect of varying the CKM parameters $|V_{ub}/V_{cb}|$ and δ_{13}. Within the SM, these parameters are determined by combining the measurements of several observables: $b \to u\ell\bar{\nu}$ semileptonic decays, ε_K, Δm_{B_d}, $\Delta m_{B_s}/\Delta m_{B_d}$, and the time-dependent CP asymmetry of the $B \to J/\psi K_S$ decay. However, in the present case we have shown that there can be significant SUSY contributions to these observables, especially for ε_K. In such a case the allowed range of δ_{13} given by the measured value of ε_K is different from that in the SM case, and then this change affects the other observables. As for $|V_{ub}/V_{cb}|$, we have no change since the $b \to u\ell\bar{\nu}$ decay is dominated by the tree-level SM amplitude.

We show how this effect will be observed in Fig. 14, where the possible region in space of $\Delta m_{B_s}/\Delta m_{B_d}$ and the time-dependent CP asymmetry of $B \to J/\psi K_S$ are presented. In this figure, we vary $|V_{ub}/V_{cb}|$ and δ_{13} within the ranges $0.08 < |V_{ub}/V_{cb}| < 0.1$ and $0 < \delta_{13} < 360°$. The dotted lines in each plot show the SM values of $\Delta m_{B_s}/\Delta m_{B_d}$ and $A_{CP}(B$

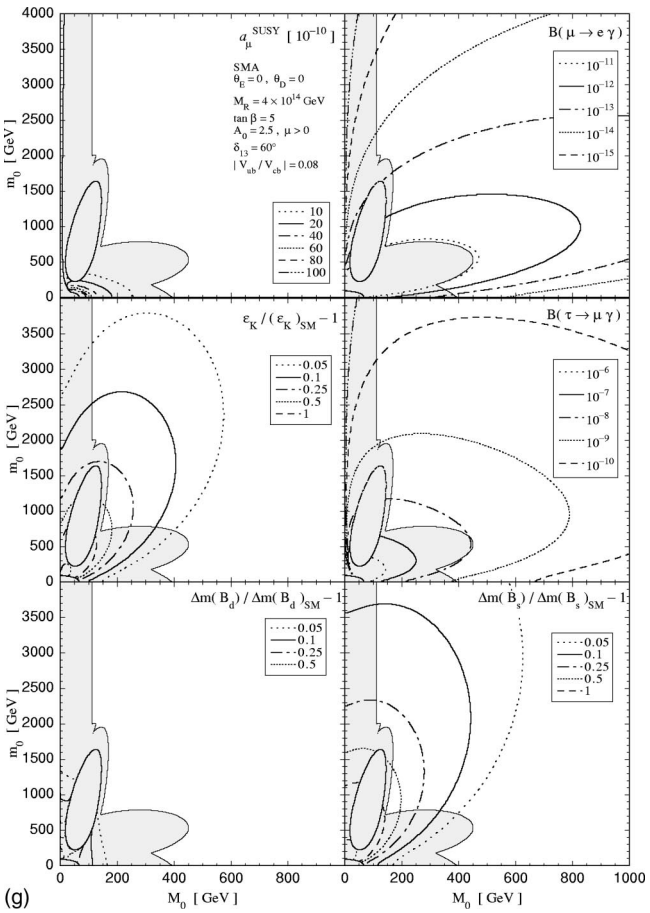

FIG. 11. (*Continued*).

$\to J/\psi K_S$) for the whole range of δ_{13} and $|V_{ub}/V_{cb}| = 0.1$ (outer line) and 0.08 (inner line). The shaded region is allowed in the SM case. We impose the constraints from the measured values of $\varepsilon_K = 2.28 \times 10^{-3}$ and $\Delta m_{B_d} = 0.482$ ps^{-1} and from the lower limit of $\Delta m_{B_s} > 14.3$ ps^{-1}. In the calculation of ε_K, Δm_{B_d}, and Δm_{B_s} we fix the bag parameters and the decay constant of the B meson

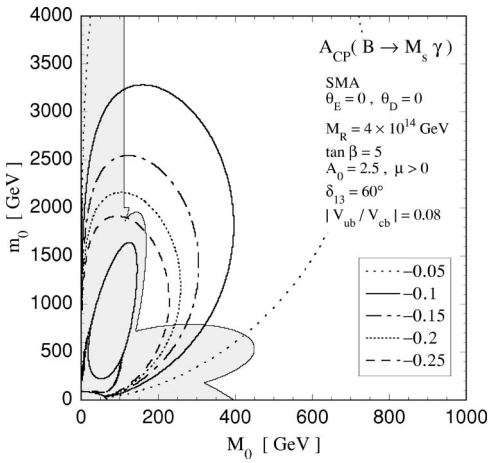

FIG. 12. Contour plot of the time-dependent CP asymmetry of $B \to M_s \gamma$ decay with the same parameter set as Fig. 11(g).

f_{B_d,B_s} as given in Table V [36]. When we impose the experimental constraints, we allow $\pm 15\%$ and $\pm 40\%$ deviations for ε_K and Δm_{B_d}, respectively, in order to take theoretical uncertainties in the bag parameters into account. Since this uncertainty is expected to be reduced in the ratio $\Delta m_{B_s}/\Delta m_{B_d}$, we use the lower limit of the ratio $\Delta m_{B_s}/\Delta m_{B_d}$ instead of Δm_{B_s} itself.

Figure 14(a) shows the result with the same parameter set as Fig. 11(a) except that A_0 is scanned within $-5 < A_0 < +5$ (see Table III). As shown in Figs. 11(a) and (b), the SUSY contributions to B_d-$\overline{B_d}$ mixing and B_s-$\overline{B_s}$ mixing are quite small in this case so that the allowed region lies between the dotted lines. The difference of the allowed regions from the SM values comes from the fact that the SUSY contribution to ε_K can be as large as 50% of the SM value, as can be seen in Fig. 13.

In Fig. 14(b) we take $\theta_D = 45°$ as in Fig. 11(c) and A_0 is scanned within $-5 < A_0 < +5$. In this case the enhancement of ε_K is more significant than in the $\theta_D = 0$ case. Consequently a region with smaller δ_{13} is now allowed and hence a smaller $A_{CP}(B \to J/\psi K_S) \sim 0.4$ is possible, compared to the SM value $A_{CP}(B \to J/\psi K_S) \sim 0.7$. At the same time $\Delta m_{B_s}/\Delta m_{B_d}$ can be as large as 60.

Figure 14(c) is the case corresponding to Fig. 11(g) with $-5 < A_0 < +5$. In this case the allowed region can be outside the dotted circles, since a large deviation of Δm_{B_s} is possible. On the other hand, we see that the deviation of $A_{CP}(B \to J/\psi K_S)$ from the SM value is small.

At present we have only a lower bound for Δm_{B_s} and the CP asymmetry of $B \to J/\psi K_S$ and related modes is not precise enough [35,37]. In a few years we expect that Δm_{B_s} will be measured at the Tevatron and the precision of the CP violating asymmetry will be improved to the 10% level at the Belle, BaBar, and Tevatron experiments. It is conceivable that the deviation shown in Fig. 14 will be clearly seen in these experiments.

V. CONCLUSION AND DISCUSSION

In this paper we have studied FCNC and LFV processes as well as the muon anomalous magnetic moment in the framework of SU(5) SUSY GUT with right-handed neutrinos, motivated by the large mixing angle solutions for the atmospheric and solar neutrino anomalies. In order to explain realistic mass relations for quarks and leptons, we have taken into account effects of higher dimensional operators above the GUT scale. It has been shown that there appear new mixing angles in the right-handed charged leptons and the right-handed down-type quarks due to the higher dimensional operators. We have calculated various low energy observables by changing parameters of the model, namely, SUSY parameters, neutrino parameters (LMA or SMA and M_R), and the above new mixing angles. We have shown that, within the current experimental bound of $B(\mu \to e\,\gamma)$, large SUSY contributions are possible either in the muon anomalous magnetic moment or in ε_K. The parameter regions that have a large correction in one case are different from those in

TABLE IV. Summary of the SUSY contributions to the observables in Fig. 11. "√" shows that some parameter region is excluded by the $\mu \to e\,\gamma$ constraint and hence the branching ratio can be just below the present upper bound. "–" means that the SUSY contribution is negligible.

	(a)	(b)	(c)	(d)	(e)	(f)	(g)
$a_\mu^{\rm SUSY}$ (10^{-10})	$\lesssim 50$	$\lesssim 50$	$\lesssim 10$	–	–	$\lesssim 50$	–
$B(\mu \to e\,\gamma)$	√	√	√	$\lesssim 10^{-13}$	√	$\lesssim 10^{-13}$	√
$B(\tau \to \mu\,\gamma)$	$\lesssim 10^{-9}$	$\lesssim 10^{-9}$	$\lesssim 10^{-9}$	$\lesssim 10^{-10}$	$\lesssim 10^{-9}$	$\lesssim 10^{-8}$	$\lesssim 10^{-7}$
$\varepsilon_K/(\varepsilon_K)_{\rm SM}-1$	$\lesssim 0.1$	$\lesssim 0.5$	$\lesssim 1$	$\lesssim 0.05$	$\lesssim 0.5$	–	$\lesssim 0.5$
$\Delta m_{B_d}/(\Delta m_{B_d})_{\rm SM}-1$	–	–	–	–	–	–	–
$\Delta m_{B_s}/(\Delta m_{B_s})_{\rm SM}-1$	–	–	–	–	$\lesssim 0.05$	–	$\lesssim 1$

the other case. In the former case, the favorable value of the recent result of the BNL E821 experiment can be accommodated. In the latter case, the allowed region of the Kobayashi-Maskawa phase can be different from the predictions within the SM, and therefore measurements of the CP asymmetry of the $B \to J/\psi K_S$ mode and Δm_{B_s} can discriminate this case from the SM. We also show that the $\tau \to \mu\gamma$ branching ratio can be close to the current experimental upper bound and the mixing-induced CP asymmetry of the radiative B decay can be enhanced in the case where the neutrino parameters correspond to the small mixing angle MSW solution.

Finally there are several remarks.

In this paper we have neglected the constraint from the nucleon decay. If we take the minimal model for the Higgs sector at the GUT scale, it is likely that the nucleon decay experiments exclude most of the parameter space even if the squark mass is multi-TeV [38]. It is known, however, that there are several ways to suppress the nucleon decay without changing the flavor signals discussed here [39].

For LFV search, $\mu \to eee$ decay and μ-e conversion in a muonic atom are also promising experimentally [40]. The rates of these processes have simple relations with $B(\mu \to e\,\gamma)$ if the photonic operator Eq. (32) gives the dominant contribution [17,41]:

$$\frac{B(\mu^+ \to e^+ e^+ e^-)}{B(\mu^+ \to e^+ \gamma)} \approx \frac{\alpha}{3\pi}\left[\log\frac{m_\mu^2}{m_e^2} - \frac{11}{4}\right] \approx 0.006, \tag{41a}$$

$$\frac{B(\mu^- N \to e^- N)}{B(\mu^+ \to e^+ \gamma)} \approx \frac{B(A,Z)}{428}, \tag{41b}$$

where $B(A,Z)$ represents the rate dependence on the mass number A and the atomic number Z of the target nucleus:

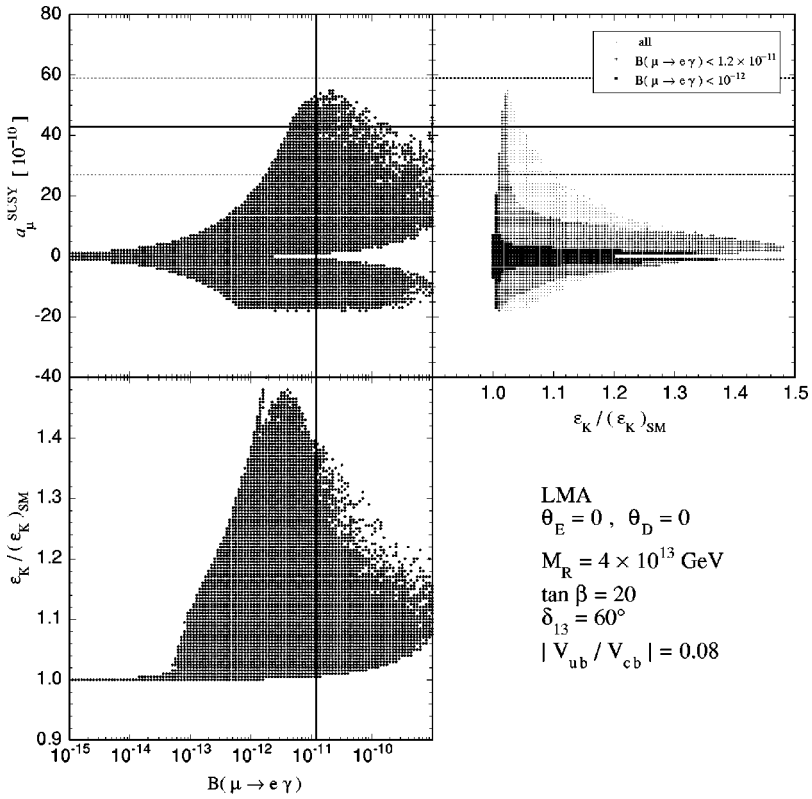

FIG. 13. Correlation among $a_\mu^{\rm SUSY}$, $B(\mu \to e\gamma)$, and ε_K. The vertical line shows the experimental upper bound $B(\mu \to e\gamma) < 1.2 \times 10^{-11}$ [34] and the horizontal solid and dotted lines show the E821-favored region $a_\mu^{\rm SUSY} = (43 \pm 16) \times 10^{-10}$ [1].

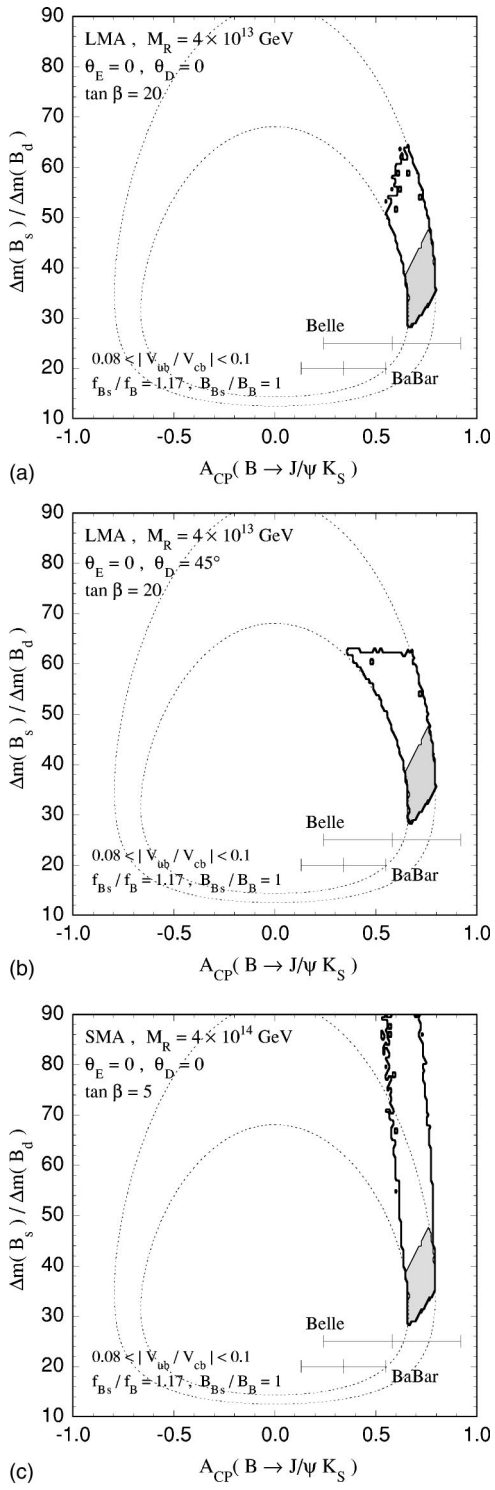

FIG. 14. Allowed region in $\Delta m_{B_s}/\Delta m_{B_d}$-$A_{CP}(B\to J/\psi K_S)$ plane. δ_{13} and $|V_{ub}/V_{cb}|$ are varied and constraints from ε_K, Δm_{B_d}, and $\Delta m_{B_s}/\Delta m_{B_d}$ are imposed. 1σ ranges of the CP asymmetry from Belle and BaBar experiments are also shown [35].

$B(A,Z)\approx 1.1$ for ^{27}Al, $B(A,Z)\approx 1.8$ for ^{48}Ti, and $B(A,Z)\approx 1.25$ for ^{208}Pb. These relations hold in our case also.

We also calculated the $\tau\to e\gamma$ branching ratio. In all cases $B(\tau\to e\gamma)$ is smaller by two or three orders of magnitude than $B(\tau\to\mu\gamma)$.

TABLE V. Decay constants and bag parameters for B^0-$\overline{B^0}$ and K^0-$\overline{K^0}$ mixing matrix elements used in the numerical calculation [36].

f_{B_d}	f_{B_s}/f_{B_d}	B_B	$(B_B)^S_{RL}$	$(B_B)^S_{RL}{}'$	B_K	$(B_K)^S_{RL}$	$(B_K)^S_{RL}{}'$
210 MeV	1.17	0.8	0.8	0.8	0.69	1.03	0.73

As shown in Figs. 11(a) and (e), the flavor mixing effect due to the neutrino Yukawa coupling is enhanced (suppressed) for large (small) M_R since the neutrino Yukawa coupling constants are proportional to $\sqrt{M_R}$ for given neutrino masses. When we take a small value of M_R, such as $M_R \lesssim 10^{10}$ GeV, the contributions of y_ν in m_L^2 and m_D^2 given in Eqs. (25c) and (25d) are suppressed and hence the SUSY contribution to ε_K becomes smaller than $\sim 10\%$. Even in this case, however, there are contributions to the $\mu\to e\gamma$ decay amplitudes independent of the magnitude of y_ν, as shown in Eq. (33). The terms proportional to a_1^n dominate the amplitude for $\theta_{D,E}=O(1)$ and the branching ratio can be as large as the experimental upper bound in some parameter regions.

We have assumed the 1-3 element of the MNS matrix to be vanishing. However, the present experimental upper bound is given as $\sin^2 2\theta_{13}<0.1$ [23]. When a nonvanishing θ_{13} is introduced, $\mu\to e\gamma$ and ε_K are generally enhanced since the loop diagrams including the third-generation squarks/sleptons in the internal lines give large contributions [17]. Consequently, the constraint from the upper bound of $B(\mu\to e\gamma)$ is significant even in the SMA case. In the allowed region, $a_\mu^{\rm SUSY}$ and the SUSY contributions to Δm_{B_d} and Δm_{B_s} are smaller than those in the $\theta_{13}=0$ case shown in Fig. 11. We see that the large deviation of $\Delta m_{B_s}/\Delta m_{B_d}$ outside the dotted lines given in Fig. 14(c) disappears when we take $\sin^2 2\theta_{13}\gtrsim 0.001$, and the corresponding plot looks similar to Fig. 14(b).

Let us now discuss the validity of the simplification imposed in the mixing matrices V_D and V_E. We have numerically checked that, when we require $|(\kappa_d)_{ij}|<4$, for example, the mixing angles for the second-third and first-third generation mixings are restricted to be smaller than $\sim 15°$ for the $\tan\beta=20$ case. In this case $B(\mu\to e\gamma)$ varies within a range that is several times larger than those shown in Fig. 9. In addition to the mixing angles, CP violating complex phases of $O(1)$ can be introduced in V_D and V_E. It turns out that the SUSY contributions to ε_K can be twice as large as those given in Fig. 10. These complex phases also contributes to the electric dipole moments (EDMs) of the neutron (d_n) and the electron (d_e). We calculated EDMs and obtained the result that $|d_n|\lesssim 10^{-26}$ e cm and $|d_e|\lesssim 10^{-27}$ e cm for $m_0=600$ GeV, $M_0=300$ GeV, and $A_0=0$. Thus the EDMs can be close to the present upper bounds $|d_n|<6.3\times 10^{-26}$ e cm [42] and $|d_e|<4.0\times 10^{-27}$ e cm [43].

As discussed above, if we relax the simple assumptions for the mixing matrices V_D, V_E, and $V_{\rm MNS}$, typical patterns of the deviation from the SM can be summarized in the following way. (1) $B(\mu\to e\gamma)$ can be close to 10^{-11} and the

deviation in the $\Delta m_{B_s}/\Delta m_{B_d}$-$A_{CP}(B\to J/\psi K_S)$ plane appears like Fig. 14(b). In this case, $a_\mu^{\rm SUSY}$ is quite small and the SUSY contribution does not saturate the observed discrepancy of a_μ. (2) $a_\mu^{\rm SUSY}$ is compatible with the E821 result and $B(\mu\to e\,\gamma)$ can be as large as 10^{-11}. However, no deviation may be seen in ε_K or the B_d-$\overline{B_d}$ and B_s-$\overline{B_s}$ mixings in this case. From these observations we can conclude that it is important to search for new physics effects in the ongoing and near-future experiments, namely, the BNL muon $g-2$ experiment, $\mu\to e\,\gamma$ and $\mu-e$ conversion experiments [44,45], and B physics experiments at B factories and the Tevatron. By combining results obtained in these experiments we may be able to get some insights into interactions at the GUT or right-handed neutrino scales.

ACKNOWLEDGMENTS

The work of Y.O. was supported in part by a Grant-in-Aid of the Ministry of Education, Culture, Sports, Science and Technology, Government of Japan (No. 09640381), priority area ''Supersymmetry and Unified Theory of Elementary Particles'' (No. 707), and ''Physics of CP violation'' (No. 09246105).

APPENDIX A: RGE AND MATCHING CONDITION AT THE GUT SCALE

In this appendix we show the details of our numerical calculation taking account of the effects of higher dimensional operators. An outline of the calculation is as follows.

We solve the renormalization group equations (RGEs) for the gauge and Yukawa coupling constants between the EW scale and the GUT scale. The neutrino Yukawa coupling constants are calculated with Eq. (28) at the Majorana mass scale.

At the GUT scale, the coupling constants in the superpotential of the SU(5)RN SUSY GUT are determined from the Yukawa coupling constants for quarks and leptons using the matching condition explained in Sec. A 2 below. Then we solve the RGEs for these constants between the GUT scale and the Planck scale.

At the Planck scale, we set the boundary conditions for the SUSY breaking parameters as Eq. (19) and solve the RGEs for these parameters between the Planck scale and the EW scale.

The RGEs for the MSSM and MSSMRN are given, for example, in Refs. [6,17] and we show the RGEs for the SU(5)RN SUSY GUT in Sec. A 1. In Sec. A 2 we explain the matching condition at the GUT scale, taking account of the higher dimensional terms in the Kähler potential.

1. RGE for the SU(5) SUSY GUT with right-handed neutrino

In this subsection we show one-loop RGEs for the SU(5)RN SUSY GUT. In the derivation of the RGEs, we only take account of diagrams in which the higher dimensional operators are inserted at most one time. In this approximation, the quadratic divergence does not appear in the calculation.

The RGEs for the SU(5) gauge coupling constant g_5 and the gaugino mass parameter M_5 are given by

$$(4\pi)^2 M\frac{d}{dM}g_5 = b_5 g_5^3, \tag{A1a}$$

$$(4\pi)^2 M\frac{d}{dM}M_5 = 2b_5 g_5^2 M_5, \tag{A1b}$$

where M is the renormalization scale. The coefficient of the beta function is given as $b_5=-3$ for minimal field content.

The RGEs for the coupling constants in the superpotentials Eqs. (1) and (6) are represented as follows:

$$(4\pi)^2 M\frac{d}{dM}(\lambda_u)_{ij} = (\lambda_u)_{kj}(\Theta_T)^k{}_i + (\lambda_u)_{ik}(\Theta_T)^k{}_j + (\lambda_u)_{ij}\Theta_H, \tag{A2a}$$

$$(4\pi)^2 M\frac{d}{dM}(\lambda_d)_{ij} = (\lambda_d)_{kj}(\Theta_{\overline{F}})^k{}_i + (\lambda_d)_{ik}(\Theta_T)^k{}_j + (\lambda_d)_{ij}\Theta_{\overline{H}}, \tag{A2b}$$

$$(4\pi)^2 M\frac{d}{dM}(\lambda_\nu)_{ij} = (\lambda_\nu)_{kj}(\Theta_{\overline{N}})^k{}_i + (\lambda_\nu)_{ik}(\Theta_{\overline{F}})^k{}_j + (\lambda_\nu)_{ij}\Theta_H, \tag{A2c}$$

$$(4\pi)^2 M\frac{d}{dM}(\kappa_u^{\pm})_{ij} = (\kappa_u^{\pm})_{kj}(\Theta_T)^k{}_i + (\kappa_u^{\pm})_{ik}(\Theta_T)^k{}_j + (\kappa_u^{\pm})_{ij}(\Theta_H+\Theta_\Sigma), \tag{A2d}$$

$$(4\pi)^2 M\frac{d}{dM}(\kappa_d)_{ij} = (\kappa_d)_{kj}(\Theta_{\overline{F}})^k{}_i + (\kappa_d)_{ik}(\Theta_T)^k{}_j + (\kappa_d)_{ij}(\Theta_{\overline{H}}+\Theta_\Sigma), \tag{A2e}$$

$$(4\pi)^2 M\frac{d}{dM}(\overline{\kappa}_d)_{ij} = (\overline{\kappa}_d)_{kj}(\Theta_{\overline{F}})^k{}_i + (\overline{\kappa}_d)_{ik}(\Theta_T)^k{}_j + (\overline{\kappa}_d)_{ij}(\Theta_{\overline{H}}+\Theta_\Sigma), \tag{A2f}$$

$$(4\pi)^2 M\frac{d}{dM}(\kappa_\nu)_{ij} = (\kappa_\nu)_{kj}(\Theta_{\overline{N}})^k{}_i + (\kappa_\nu)_{ik}(\Theta_T)^k{}_j + (\kappa_\nu)_{ij}(\Theta_H+\Theta_\Sigma), \tag{A2g}$$

where the Θ's are given by

$$(\Theta_T)^i{}_j = 2(\lambda_d^\dagger)^{ik}(\lambda_d)_{kj} + 3(\lambda_u^\dagger)^{ik}(\lambda_u)_{kj} - \frac{36}{5}g_5^2\delta^i_j, \tag{A3a}$$

$$(\Theta_{\overline{F}})^i{}_j = 4(\lambda_d^*)^{ik}(\lambda_d^T)_{kj} + (\lambda_\nu^\dagger)^{ik}(\lambda_\nu)_{kj} - \frac{24}{5}g_5^2\delta^i_j, \tag{A3b}$$

$$(\Theta_{\overline{N}})^i{}_j = 5(\lambda_\nu^*)^{ik}(\lambda_\nu^T)_{kj}, \tag{A3c}$$

$$\Theta_{\overline{H}} = 4\mathrm{Tr}(\lambda_d^\dagger \lambda_d) - \frac{24}{5} g_5^2, \tag{A3d}$$

$$\Theta_H = \frac{3}{2}\mathrm{Tr}(\lambda_u^\dagger \lambda_u) + \mathrm{Tr}(\lambda_\nu^\dagger \lambda_\nu) - \frac{24}{5} g_5^2, \tag{A3e}$$

$$\Theta_\Sigma = -10 g_5^2. \tag{A3f}$$

The RGEs for the SUSY breaking parameters in Eq. (18) are written as follows:

$$\begin{aligned}(4\pi)^2 M\frac{d}{dM}(\tilde{\lambda}_u)_{ij} &= (\tilde{\lambda}_u)_{kj}(\Theta_T)^k{}_i + (\tilde{\lambda}_u)_{ik}(\Theta_T)^k{}_j \\ &+ (\tilde{\lambda}_u)_{ij}\Theta_H + 2\{(\lambda_u)_{kj}(\tilde{\Theta}_T)^k{}_i \\ &+ (\lambda_u)_{ik}(\tilde{\Theta}_T)^k{}_j + (\lambda_u)_{ij}\tilde{\Theta}_H\},\end{aligned} \tag{A4a}$$

$$\begin{aligned}(4\pi)^2 M\frac{d}{dM}(\tilde{\lambda}_d)_{ij} &= (\tilde{\lambda}_d)_{kj}(\Theta_{\overline{F}})^k{}_i + (\tilde{\lambda}_d)_{ik}(\Theta_T)^k{}_j \\ &+ (\tilde{\lambda}_d)_{ij}\Theta_{\overline{H}} + 2\{(\lambda_d)_{kj}(\tilde{\Theta}_{\overline{F}})^k{}_i \\ &+ (\lambda_d)_{ik}(\tilde{\Theta}_T)^k{}_j + (\lambda_d)_{ij}\tilde{\Theta}_{\overline{H}}\},\end{aligned} \tag{A4b}$$

$$\begin{aligned}(4\pi)^2 M\frac{d}{dM}(\tilde{\lambda}_\nu)_{ij} &= (\tilde{\lambda}_\nu)_{kj}(\Theta_{\overline{N}})^k{}_i + (\tilde{\lambda}_\nu)_{ik}(\Theta_{\overline{F}})^k{}_j \\ &+ (\tilde{\lambda}_\nu)_{ij}\Theta_H + 2\{(\lambda_\nu)_{kj}(\tilde{\Theta}_{\overline{N}})^k{}_i \\ &+ (\lambda_\nu)_{ik}(\tilde{\Theta}_{\overline{F}})^k{}_j + (\lambda_\nu)_{ij}\tilde{\Theta}_H\},\end{aligned} \tag{A4c}$$

$$\begin{aligned}(4\pi)^2 M\frac{d}{dM}(\tilde{\kappa}_u^\pm)_{ij} &= (\tilde{\kappa}_u^\pm)_{kj}(\Theta_T)^k{}_i + (\tilde{\kappa}_u^\pm)_{ik}(\Theta_T)^k{}_j \\ &+ (\tilde{\kappa}_u^\pm)_{ij}(\Theta_\Sigma + \Theta_H) \\ &+ 2\{(\kappa_u^\pm)_{kj}(\tilde{\Theta}_T)^k{}_i + (\kappa_u^\pm)_{ik}(\tilde{\Theta}_T)^k{}_j \\ &+ (\kappa_u^\pm)_{ij}(\tilde{\Theta}_\Sigma + \tilde{\Theta}_H)\},\end{aligned} \tag{A4d}$$

$$\begin{aligned}(4\pi)^2 M\frac{d}{dM}(\tilde{\kappa}_d)_{ij} &= (\tilde{\kappa}_d)_{kj}(\Theta_{\overline{F}})^k{}_i + (\tilde{\kappa}_d)_{ik}(\Theta_T)^k{}_j \\ &+ (\tilde{\kappa}_d)_{ij}(\Theta_\Sigma + \Theta_{\overline{H}}) + 2\{(\kappa_d)_{kj}(\tilde{\Theta}_{\overline{F}})^k{}_i \\ &+ (\kappa_d)_{ik}(\tilde{\Theta}_T)^k{}_j + (\kappa_d)_{ij}(\tilde{\Theta}_\Sigma + \tilde{\Theta}_{\overline{H}})\},\end{aligned} \tag{A4e}$$

$$\begin{aligned}(4\pi)^2 M\frac{d}{dM}(\overline{\tilde{\kappa}}_d)_{ij} &= (\overline{\tilde{\kappa}}_d)_{kj}(\Theta_{\overline{F}})^k{}_i + (\overline{\tilde{\kappa}}_d)_{ik}(\Theta_T)^k{}_j \\ &+ (\overline{\tilde{\kappa}}_d)_{ij}(\Theta_\Sigma + \Theta_{\overline{H}}) + 2\{(\overline{\kappa}_d)_{kj}(\tilde{\Theta}_{\overline{F}})^k{}_i \\ &+ (\overline{\kappa}_d)_{ik}(\tilde{\Theta}_T)^k{}_j + (\overline{\kappa}_d)_{ij}(\tilde{\Theta}_\Sigma + \tilde{\Theta}_{\overline{H}})\},\end{aligned} \tag{A4f}$$

$$\begin{aligned}(4\pi)^2 M\frac{d}{dM}(\tilde{\kappa}_\nu)_{ij} &= (\tilde{\kappa}_\nu)_{kj}(\Theta_{\overline{N}})^k{}_i + (\tilde{\kappa}_\nu)_{ik}(\Theta_{\overline{F}})^k{}_j \\ &+ (\tilde{\kappa}_\nu)_{ij}(\Theta_\Sigma + \Theta_H), + 2\{(\kappa_\nu)_{kj}(\tilde{\Theta}_{\overline{N}})^k{}_i \\ &+ (\kappa_\nu)_{ik}(\tilde{\Theta}_{\overline{F}})^k{}_j + (\kappa_\nu)_{ij}(\tilde{\Theta}_\Sigma + \tilde{\Theta}_H)\},\end{aligned} \tag{A4g}$$

$$\begin{aligned}(4\pi)^2 M\frac{d}{dM}(m_T^2)^i{}_j &= (\Theta_T)^i{}_k(m_T^2)^k{}_j + (m_T^2)^i{}_k(\Theta_T)^k{}_j \\ &+ 2[3(\lambda_u^\dagger)^{ik}\{(m_T^{2T})_k{}^l + (m_H^2)\delta_k^l\}(\lambda_u)_{lj} \\ &+ 2(\lambda_d^\dagger)^{ik}\{(m_{\overline{F}}^{2T})_k{}^l + (m_{\overline{H}}^2)\delta_k^l\}(\lambda_d)_{lj} \\ &+ 3(\tilde{\lambda}_u^\dagger)^{ik}(\tilde{\lambda}_u)_{kj} + 2(\tilde{\lambda}_d^\dagger)^{ik}(\tilde{\lambda}_d)_{kj}] \\ &+ \frac{72}{5} g_5^2\{(m_T^2)^i{}_j - 2|M_5|^2\delta_j^i\},\end{aligned} \tag{A4h}$$

$$\begin{aligned}(4\pi)^2 M\frac{d}{dM}(m_{\overline{F}}^2)^i{}_j &= (\Theta_{\overline{F}})^i{}_k(m_{\overline{F}}^2)^k{}_j + (m_{\overline{F}}^2)^i{}_k(\Theta_{\overline{F}})^k{}_j \\ &+ 2[4(\lambda_d^*)^{ik}\{(m_T^{2T})_k{}^l + (m_{\overline{H}}^2)\delta_k^l\} \\ &\times(\lambda_d^T)_{lj} + (\lambda_\nu^\dagger)^{ik}\{(m_N^{2T})_k{}^l + (m_H^2)\delta_k^l\} \\ &\times(\lambda_\nu)_{lj} + 4(\tilde{\lambda}_d^*)^{ik}(\tilde{\lambda}_d^T)_{kj} \\ &+ (\tilde{\lambda}_\nu^\dagger)^{ik}(\tilde{\lambda}_\nu)_{kj}] + \frac{48}{5} g_5^2\{(m_{\overline{F}}^2)^i{}_j \\ &- 2|M_5|^2\delta_j^i\},\end{aligned} \tag{A4i}$$

$$\begin{aligned}(4\pi)^2 M\frac{d}{dM}(m_{\overline{N}}^2)^i{}_j &= (\Theta_{\overline{N}})^i{}_k(m_{\overline{N}}^2)^k{}_j + (m_{\overline{N}})^2)^i{}_k(\Theta_{\overline{N}})^k{}_j \\ &+ 2[5(\lambda_\nu^*)^{ik}\{(m_{\overline{F}}^{2T})_k{}^l + (m_H^2)\delta_k^l\} \\ &\times(\lambda_\nu^T)_{lj} + 5(\tilde{\lambda}_\nu^*)^{ik}(\tilde{\lambda}_\nu^T)_{kj}],\end{aligned} \tag{A4j}$$

$$\begin{aligned}(4\pi)^2 M\frac{d}{dM}m_H^2 &= 2\Theta_H m_H^2 + 2\{6\mathrm{Tr}(\lambda_u^\dagger m_T^{2T}\lambda_u) \\ &+ \mathrm{Tr}(\lambda_\nu^\dagger m_{\overline{N}}^{2T}\lambda_\nu) + \mathrm{Tr}(\lambda_\nu^* m_{\overline{F}}^{2T}\lambda_\nu^T) \\ &+ 3\mathrm{Tr}(\tilde{\lambda}_u^\dagger\tilde{\lambda}_u) + \mathrm{Tr}(\tilde{\lambda}_\nu^\dagger\tilde{\lambda}_\nu)\} \\ &+ \frac{48}{5} g_5^2(m_H^2 - 2|M_5|^2),\end{aligned} \tag{A4k}$$

$$\begin{aligned}(4\pi)^2 M\frac{d}{dM}(m_{\overline{H}}^2) &= 2\,\Theta_{\overline{H}} m_{\overline{H}}^2 + 2\{4\mathrm{Tr}(\lambda_d^* m_T^{2T}\lambda_d^T) \\ &+ 4\mathrm{Tr}(\lambda_d^\dagger m_{\overline{F}}^{2T}\lambda_d) + 4\mathrm{Tr}(\tilde{\lambda}_d^*\tilde{\lambda}_d^T)\} \\ &+ \frac{48}{5} g_5^2(m_{\overline{H}}^2 - 2|M_5|^2),\end{aligned} \tag{A4l}$$

where the $\tilde{\Theta}$'s are given by

$$(\tilde{\Theta}_T)^i{}_j = 2(\lambda_d^\dagger)^{ik}(\tilde{\lambda}_d)_{kj} + 3(\lambda_u^\dagger)^{ik}(\tilde{\lambda}_u)_{kj} - \frac{36}{5} g_5^2 M_5 \delta^i_j, \tag{A5a}$$

$$(\tilde{\Theta}_{\overline{F}})^i{}_j = 4(\lambda_d^*)^{ik}(\tilde{\lambda}_d^T)_{kj} + (\lambda_\nu^\dagger)^{ik}(\tilde{\lambda}_\nu)_{kj} - \frac{24}{5} g_5^2 M_5 \delta^i_j, \tag{A5b}$$

$$(\tilde{\Theta}_{\overline{N}})^i{}_j = 5(\lambda_\nu^*)^{ik}(\tilde{\lambda}_\nu^T)_{kj}, \tag{A5c}$$

$$\tilde{\Theta}_{\overline{H}} = 4\mathrm{Tr}(\lambda_d^\dagger \tilde{\lambda}_d) - \frac{24}{5} g_5^2 M_5, \tag{A5d}$$

$$\tilde{\Theta}_H = \frac{3}{2}\mathrm{Tr}(\lambda_u^\dagger \tilde{\lambda}_u) + \mathrm{Tr}(\lambda_\nu^\dagger \tilde{\lambda}_\nu) - \frac{24}{5} g_5^2 M_5, \tag{A5e}$$

$$\tilde{\Theta}_\Sigma = -10 g_5^2 M_5. \tag{A5f}$$

2. Matching conditions at the GUT scale

In this subsection we show the matching conditions between the SU(5)RN SUSY GUT and the MSSMRN at the GUT scale taking account of the dimension five terms in the Kähler potential. Although we include only the renormalizable terms in the Kähler potential at the Planck scale, higher dimensional terms are induced by the renormalization effects between the Planck scale and the GUT scale, because we introduce the higher dimensional operators in the superpotential. In order to simplify the treatment, we use the logarithmic approximation for induced terms in the Kähler potential. For other coupling constants, we explicitly solve the RGEs in the previous subsection.

Up to dimension five terms, the corrections for the Kähler potential in the present model are parametrized as follows:

$$\begin{aligned}\Delta\mathcal{K}_{\mathrm{SU(5)RN}} = \frac{1}{M_X}\{&(\bar{k}_T)^i{}_j (T_i^\dagger)_{ab}(\Sigma)^b{}_c (T^j)^{ca} \\ &+ (\bar{k}_{\overline{F}})^i{}_j (\overline{F}_i^\dagger)^a (\Sigma)^b{}_a (\overline{F}_j)_b + \bar{k}_H (H^\dagger)_a (\Sigma)^a{}_b (H)^b \\ &+ \bar{k}_{\overline{H}} (\overline{H}^\dagger)^a (\Sigma)^b{}_a (\overline{H})_b\} + \mathrm{H.c.},\end{aligned} \tag{A6}$$

where we include SUSY breaking parts in the coupling constants using the spurion method as follows:

$$\bar{k}_X = k_X + \hat{k}_X \theta^2 + \check{k}_X \bar{\theta}^2 + \tilde{k}_X \theta^2 \bar{\theta}^2 \qquad (X = T, \overline{F}, H, \overline{H}). \tag{A7}$$

At the Planck scale, we assume all the components of Eq. (A7) are zero. These coupling constants are induced from the renormalization between the Planck scale and the GUT scale. In the logarithmic approximation, the k's at the GUT scale are given by

$$\begin{aligned}(k_T)^i{}_j \approx -2\{&(\lambda_u^\dagger)^{ik}(\kappa_u^+)_{kj} - 5(\lambda_u^\dagger)^{ik}(\kappa_u^-)_{kj} + (\lambda_d^\dagger)^{ik}(\kappa_d)_{kj} \\ &+ (\lambda_d^\dagger)^{ik}(\bar{\kappa}_d)_{kj}\} t_G,\end{aligned} \tag{A8a}$$

$$\begin{aligned}(k_{\overline{F}})^i{}_j \approx -2\{&(\lambda_d^*)^{ik}(\kappa_d)_{jk} - 4(\lambda_d^*)^{ik}(\bar{\kappa}_d)_{jk} \\ &- (\lambda_\nu^\dagger)^{ik}(\kappa_\nu)_{kj}\} t_G,\end{aligned} \tag{A8b}$$

$$k_H \approx -2\{3\mathrm{Tr}(\lambda_u^\dagger \kappa_u) - \mathrm{Tr}(\lambda_\nu^\dagger \kappa_\nu)\} t_G, \tag{A8c}$$

$$k_{\overline{H}} \approx -2\{\mathrm{Tr}(\lambda_d^\dagger \kappa_d) - 4\mathrm{Tr}(\lambda_d^\dagger \bar{\kappa}_d)\} t_G. \tag{A8d}$$

In the same approximation, $\hat{k}_X$, $\check{k}_X$, and $\tilde{k}_X$ at the GUT scale are proportional to k_X as follows:

$$\hat{k}_X \approx m_0 (A_0 + \Delta A_0) k_X, \tag{A9a}$$

$$\check{k}_X \approx m_0 A_0 k_X, \tag{A9b}$$

$$\tilde{k}_X \approx m_0^2 \{A_0^* (A_0 + \Delta A_0) + 2\} k_X \qquad (X = T, \overline{F}, H, \overline{H}). \tag{A9c}$$

The dimension five terms in Eq. (A6) modify the normalization of the Kähler potential after the SU(5) symmetry breaking. In order to obtain the correct normalization up to $O(\xi)$, we introduce the following new chiral superfields:

$$\begin{aligned}(T^{i\prime})^{ab} = (T^i)^{ab} + \frac{1}{M_X}\{&(k_T)^i{}_j + \theta^2 (\hat{k}_T)^i{}_j\}\{(\Sigma)^a{}_c (T^j)^{cb} \\ &- (\Sigma)^b{}_c (T^j)^{ca}\},\end{aligned} \tag{A10a}$$

$$(\overline{F}^{i\prime})_a = (\overline{F}^i)_a + \frac{1}{M_X}\{(k_{\overline{F}})^i{}_j + \theta^2 (\hat{k}_{\overline{F}})^i{}_j\}(\Sigma)^b{}_a (\overline{F}^j)_b, \tag{A10b}$$

$$(H')^a = (H)^a + \frac{1}{M_X}(k_H + \theta^2 \hat{k}_H)(\Sigma)^a{}_b H^b, \tag{A10c}$$

$$(\overline{H}')_a = (\overline{H})_a + \frac{1}{M_X}(k_{\overline{H}} + \theta^2 \hat{k}_{\overline{H}})(\Sigma)^b{}_a (\overline{H})_b. \tag{A10d}$$

Substituting these superfields for Eqs. (1) and (6), we can define the coupling constants in terms of the new chiral superfields as follows:

$$\begin{aligned}(\kappa_u^{+\prime})_{ij} = (\kappa_u^+)_{ij} - \frac{1}{2}(\lambda_u)_{ik}(k_T)^k{}_j - \frac{1}{2}(\lambda_u)_{kj}(k_T)^k{}_i \\ + (\lambda_u)_{ij} k_H,\end{aligned} \tag{A11a}$$

$$(\kappa_u^{-\prime})_{ij} = (\kappa_u^-)_{ij} + \frac{1}{2}(\lambda_u)_{ik}(k_T)^k{}_j - \frac{1}{2}(\lambda_u)_{kj}(k_T)^k{}_i, \tag{A11b}$$

$$(\kappa_d{}')_{ij} = (\kappa_d)_{ij} - (\lambda_d)_{ik}(k_T)^k{}_j - (\lambda_d)_{kj}(k_{\overline{F}})^k{}_i, \tag{A11c}$$

$$(\bar{\kappa}_d{}')_{ij} = (\bar{\kappa}_d)_{ij} - (\lambda_d)_{ik}(k_T)^k{}_j - (\lambda_d)_{ij} k_{\overline{H}}, \tag{A11d}$$

$$(\kappa_\nu{}')_{ij} = (\kappa_\nu)_{ij} - (\lambda_\nu)_{ik}(k_{\overline{F}})^k{}_j - (\lambda_\nu)_{ij} k_H. \tag{A11e}$$

The matching conditions for the Yukawa coupling matrices for quarks and leptons are written with the above new coupling constants as follows:[1]

$$(y_u)_{ij}=(\lambda_u)_{ij}+\xi\left\{\frac{1}{2}(\kappa_u^{+\prime})_{ij}+\frac{5}{6}(\kappa_u^{-\prime})_{ij}\right\}, \tag{A12a}$$

$$(y_d)_{ij}=(\lambda_d)_{ij}+\xi\left\{\frac{1}{3}(\kappa_d{}')_{ij}-\frac{1}{2}(\bar{\kappa}_d{}')_{ij}\right\}, \tag{A12b}$$

$$(y_e)_{ij}=(\lambda_d^T)_{ij}+\xi\left\{-\frac{1}{2}(\kappa_d{}'^T)_{ij}-\frac{1}{2}(\bar{\kappa}_d{}'^T)_{ij}\right\}, \tag{A12c}$$

$$(y_\nu)_{ij}=(\lambda_\nu)_{ij}-\frac{\xi}{2}(\kappa_\nu{}')_{ij}. \tag{A12d}$$

Using Eqs. (A8)–(A12) we can relate the y's and λ's and κ's at the GUT scale. The SUSY breaking parameters are also defined in terms of the new superfields as follows:

$$(\tilde{\kappa}_u^{+\prime})_{ij}=(\tilde{\kappa}_u^{+})_{ij}-\frac{1}{2}(\tilde{\lambda}_u)_{ik}(k_T)^k{}_j-\frac{1}{2}(\tilde{\lambda}_u)_{kj}(k_T)^k{}_i+(\tilde{\lambda}_u)_{ij}k_H-\frac{1}{2}(\lambda_u)_{ik}(\hat{k}_T)^k{}_j-\frac{1}{2}(\lambda_u)_{kj}(\hat{k}_T)^k{}_i+(\lambda_u)_{ij}\hat{k}_H, \tag{A13a}$$

$$(\tilde{\kappa}_u^{-\prime})_{ij}=(\tilde{\kappa}_u^{-})_{ij}-\frac{1}{2}(\tilde{\lambda}_u)_{ik}(k_T)^k{}_j+\frac{1}{2}(\tilde{\lambda}_u)_{kj}(k_T)^k{}_i-\frac{1}{2}(\lambda_u)_{ik}(\hat{k}_T)^k{}_j+\frac{1}{2}(\lambda_u)_{kj}(\hat{k}_T)^k{}_i, \tag{A13b}$$

$$(\tilde{\kappa}_d')_{ij}=(\tilde{\kappa}_d)_{ij}-(\tilde{\lambda}_d)_{ik}(k_T)^k{}_j-(\tilde{\lambda}_d)_{kj}(k_{\overline{F}})^k{}_i-(\lambda_d)_{ik}(\hat{k}_T)^k{}_j-(\lambda_d)_{kj}(\hat{k}_{\overline{F}})^k{}_i, \tag{A13c}$$

$$(\tilde{\bar{\kappa}}_d')_{ij}=(\tilde{\bar{\kappa}}_d)_{ij}-(\tilde{\lambda}_d)_{ik}(k_T)^k{}_j-(\tilde{\lambda}_d)_{ij}k_{\overline{H}}-(\lambda_d)_{ik}(\hat{k}_T)^k{}_j-(\lambda_d)_{ij}\hat{k}_{\overline{H}}, \tag{A13d}$$

$$(\tilde{\kappa}_\nu')_{ij}=(\tilde{\kappa}_\nu)_{ij}-(\tilde{\lambda}_\nu)_{ik}(k_{\overline{F}})^k{}_j-(\tilde{\lambda}_\nu)_{ij}k_H-(\lambda_\nu)_{ik}(\hat{k}_{\overline{F}})^k{}_j-(\lambda_\nu)_{ij}\hat{k}_H, \tag{A13e}$$

$$(\tilde{k}_T')^i{}_j=(\tilde{k}_T)^i{}_j+(m_T^2)^i{}_k(k_T)^k{}_j, \tag{A13f}$$

$$(\tilde{k}_{\overline{F}}{}')^i{}_j=(\tilde{k}_{\overline{F}})^i{}_j+(m_{\overline{F}}^2)^i{}_k(k_{\overline{F}})^k{}_j, \tag{A13g}$$

$$\tilde{k}_H'=\tilde{k}_H+m_H^2k_H, \tag{A13h}$$

$$\tilde{k}_{\overline{H}}'=\tilde{k}_{\overline{H}}+m_{\overline{H}}^2k_{\overline{H}}. \tag{A13i}$$

[1]The κ's in Eqs. (7) of Sec. II should be read as those with primes if we take account of the higher dimensional terms radiatively induced in the Kähler potential.

The soft SUSY breaking parameters can be expressed using the above new coupling constants as follows:

$$(\tilde{y}_u)_{ij}=(\tilde{\lambda}_u)_{ij}+\xi\left\{\frac{1}{2}(\tilde{\kappa}_u^{+\prime})_{ij}+\frac{5}{6}(\tilde{\kappa}_u^{-\prime})_{ij}+\frac{1}{6}(\lambda_u)_{ik}(\check{k}_T^\dagger)^k{}_j-\frac{2}{3}(\lambda_u)_{kj}(\check{k}_T^\dagger)^k{}_i+\frac{1}{2}(\lambda_u)_{ij}\check{k}_H^*\right\}, \tag{A14a}$$

$$(\tilde{y}_d)_{ij}=(\tilde{\lambda}_d)_{ij}+\xi\left\{\frac{1}{3}(\tilde{\kappa}_d{}')_{ij}-\frac{1}{2}(\tilde{\bar{\kappa}}_d{}')_{ij}-\frac{1}{6}(\lambda_d)_{ik}(\check{k}_T^\dagger)^k{}_j-\frac{1}{3}(\lambda_d)_{kj}(\check{k}_{\overline{F}}^\dagger)^k{}_i+\frac{1}{2}(\lambda_d)_{ij}\check{k}_{\overline{H}}^*\right\}, \tag{A14b}$$

$$(\tilde{y}_e)_{ij}=(\tilde{\lambda}_d^T)_{ij}+\xi\left\{-\frac{1}{2}(\tilde{\kappa}_d'^T)_{ij}-\frac{1}{2}(\tilde{\bar{\kappa}}_d'^T)_{ij}+(\lambda_d^T)_{kj}(\check{k}_T^\dagger)^k{}_i+\frac{1}{2}(\lambda_d^T)_{ik}(\check{k}_{\overline{F}}^\dagger)^k{}_j+\frac{1}{2}(\lambda_d^T)_{ij}\check{k}_{\overline{H}}^*\right\}, \tag{A14c}$$

$$(\tilde{y}_\nu)_{ij}=(\tilde{\lambda}_\nu)_{ij}+\xi\left\{-\frac{1}{2}(\tilde{\kappa}_\nu')_{ij}+\frac{1}{2}(\lambda_\nu)_{ik}(\check{k}_{\overline{F}}^\dagger)^k{}_j+\frac{1}{2}(\lambda_\nu)_{ij}\check{k}_H^*\right\}, \tag{A14d}$$

$$(m_Q^2)^i{}_j=(m_T^2)^i{}_j+\frac{1}{6}\xi\{(\tilde{k}_T')^i{}_j+(\tilde{k}_T'^\dagger)^i{}_j\}, \tag{A14e}$$

$$(m_U^2)_i{}^j=(m_T^2)^j{}_i-\frac{2}{3}\xi\{(\tilde{k}_T')^j{}_i+(\tilde{k}_T'^\dagger)^j{}_i\}, \tag{A14f}$$

$$(m_E^2)_i{}^j=(m_T^2)^j{}_i+\xi\{(\tilde{k}_T')^j{}_i+(\tilde{k}_T'^\dagger)^j{}_i\}, \tag{A14g}$$

$$(m_D^2)_i{}^j=(m_{\overline{F}}^2)^j{}_i-\frac{1}{3}\xi\{(\tilde{k}_{\overline{F}}')^j{}_i+(\tilde{k}_{\overline{F}}'^\dagger)^j{}_i\}, \tag{A14h}$$

$$(m_L^2)^i{}_j=(m_{\overline{F}}^2)^i{}_j+\frac{1}{2}\xi\{(\tilde{k}_{\overline{F}}')^i{}_j+(\tilde{k}_{\overline{F}}'^\dagger)^i{}_j\}, \tag{A14i}$$

$$m_{H_1}^2=m_{\overline{H}}^2+\xi\tilde{k}_{\overline{H}}', \tag{A14j}$$

$$m_{H_2}^2=m_H^2+\xi\tilde{k}_H'. \tag{A14k}$$

Using Eqs. (A13) and (A14), we can express the soft SUSY breaking terms of the MSSMRN by the input parameters at the Planck scale, Eq. (19).

APPENDIX B: APPROXIMATE EXPRESSIONS OF THE PHOTON-PENGUIN AMPLITUDES FOR THE $\mu\to e\gamma$ PROCESS

In this appendix we show the explicit forms of the functions that appear in the approximate expressions of the

photon-penguin amplitudes given in Eq. (33). We assume the following conditions to derive the expressions.

The off-diagonal elements of the slepton mass matrices $(m_E^2)_i^{\ j}$ and $(m_L^2)^i_{\ j}$ are given by Eqs. (25b) and (25d), and they are diagonalized with good approximation in the basis where $(y_\nu)_{ij}$ and $(y_{CR})_{ij}$ in Eqs. (22) and (23) are diagonal.

In this basis, the left-right mixing mass of the slepton can be treated as perturbation to diagonalize the 6×6 charged slepton mass matrix.

The eigenvalues of the slepton mass matrices are almost degenerate and represented by $\overline{m}^2$.

With these conditions, the SUSY contributions to the photon-penguin amplitudes correspondind to Figs. 1–3 are expressed as Eq. (33). In this formula, a_2^n, a^c, and a_1^n are given by

$$a_2^n = -\frac{e}{32\pi^2}\tan\theta_W \sum_{A=1}^{4} (O_N^*)_{A1}\{(O_N)_{A2} + \tan\theta_W (O_N)_{A1}\} f_2^n\left(\frac{\overline{m}^2}{m^2_{\tilde{\chi}^0_A}}\right)\left(\frac{m_W}{\overline{m}}\right)^2\left(\frac{m_0}{\overline{m}}\right)^4 \times \frac{m_0(A_e+\frac{3}{5}\Delta A)+\mu^*\tan\beta}{\overline{m}}(3+|A_0|^2)^2 t_G(t_G+t_R), \tag{B1a}$$

$$a^c = \frac{\sqrt{2}e}{32\pi^2\cos\beta}\sum_{A=1}^{2}(O_{CL}^*)_{A2}(O_{CR})_{A1} f^c\left(\frac{\overline{m}^2}{m^2_{\tilde{\chi}^-_A}}\right)\left(\frac{m_W}{\overline{m}}\right) \times (3+|A_0|^2)(t_G+t_R), \tag{B1b}$$

$$a_1^n = -\frac{e}{32\pi^2}\tan\theta_W \sum_{A=1}^{4}(O_N^*)_{A1}\{(O_N)_{A2} + \tan\theta_W (O_N)_{A1}\} f_1^n\left(\frac{\overline{m}^2}{m^2_{\tilde{\chi}^0_A}}\right)\left(\frac{m_W}{\overline{m}}\right)^2\left(\frac{m_0}{\overline{m}}\right)\frac{3}{5}\frac{m_s}{m_\mu}\Delta A, \tag{B1c}$$

where θ_W is the Weinberg angle. $m_{\tilde{\chi}^0_A}$ and $m_{\tilde{\chi}^-_A}$ represent the masses of neutralinos and charginos, respectively, and O_N, O_{CR}, and O_{CL} are unitary matrices which are used to diagonalize the neutralino and chargino mass matrices $M_{\tilde{\chi}^0}$ and $M_{\tilde{\chi}^-}$ as follows:

$$O_N M_{\tilde{\chi}^0} O_N^T = \mathrm{diag}(m_{\tilde{\chi}^0_1}, m_{\tilde{\chi}^0_2}, m_{\tilde{\chi}^0_3}, m_{\tilde{\chi}^0_4}), \tag{B2a}$$

$$M_{\tilde{\chi}^0} = \begin{pmatrix} M_1 & 0 & -m_Z s_W\cos\beta & m_Z s_W \sin\beta \\ 0 & M_2 & m_Z c_W\cos\beta & -m_Z c_W\sin\beta \\ -m_Z s_W\cos\beta & m_Z c_W\cos\beta & 0 & -\mu \\ m_Z s_W\sin\beta & -m_Z c_W\sin\beta & -\mu & 0 \end{pmatrix}, \tag{B2b}$$

$$O_{CR} M_{\tilde{\chi}^-} O_{CL}^\dagger = \mathrm{diag}(m_{\tilde{\chi}^-_1}, m_{\tilde{\chi}^-_2}), \tag{B2c}$$

$$M_{\tilde{\chi}^-} = \begin{pmatrix} M_2 & \sqrt{2}m_W\cos\beta \\ \sqrt{2}m_W\sin\beta & \mu \end{pmatrix}, \tag{B2d}$$

where m_Z and m_W are the Z boson mass and the W boson mass, respectively, and $s_W=\sin\theta_W$ and $c_W=\cos\theta_W$. The mass functions f_2^n, f^c, and f_1^n in the above formulas are given by

$$f_2^n(x) = -\frac{x^{7/2}}{(1-x)^4}\{x^2+4x-5+2(2x+1)\ln(x)\}, \tag{B3a}$$

$$f^c(x) = -\frac{\sqrt{x}}{2x^3(1-x)^4}\{14x^3-25x^2+14x-3 - 2x^2(4x-1)\ln(x)\}, \tag{B3b}$$

$$f_1^n(x) = \frac{1}{x^4(1-x)^5}\{5x^4-37x^3+27x^2+13x-8 + 6x(7x-3)\ln(x)\}. \tag{B3c}$$

APPENDIX C: FCNC EFFECTIVE COUPLINGS IN MSSM

In this appendix we present the explicit forms of FCNC effective coupling constants for K^0-$\overline{K}^0$, B_d-$\overline{B}_d$, and B_s-$\overline{B}_s$ mixings. For K^0-$\overline{K}^0$ mixing these coupling constants are defined in Eq. (37) of Sec. III B and for B_d-$\overline{B}_d$and B_s-$\overline{B}_s$ mixings the coupling constants are given by substitution of flavor indices. In the MSSM box diagrams exchanging charged Higgs bosons, neutralinos, charginos, and gluinos can contribute to these coupling constants. We first define the following neutralino, chargino, and gluino vertices for quarks and squarks:

$$\begin{aligned}\mathcal{L}\equiv&\sum_{i=1}^{3}\sum_{A=1}^{4}\sum_{X=1}^{6}\{\overline{d_i}(N^{dL}_{iAX}P_L+N^{dR}_{iAX}P_R)\tilde{\chi}^0_A\tilde{d}_X+\overline{u_i}(N^{uL}_{iAX}P_L\\&+N^{uR}_{iAX}P_R)\tilde{\chi}^0_A\tilde{u}_X\}+\sum_{i=1}^{3}\sum_{A=1}^{2}\sum_{X=1}^{6}\{\overline{d_i}(C^{dL}_{iAX}P_L\\&+C^{dR}_{iAX}P_R)\tilde{\chi}^-_A\tilde{u}_X+\overline{u_i}(C^{uL}_{iAX}P_L+C^{uR}_{iAX}P_R)\tilde{\chi}^-_A\tilde{d}_X\}\\&+\sum_{i=1}^{3}\sum_{X=1}^{6}\sum_{a=1}^{8}\{\overline{d_i}(\Gamma^{dL}_{iX}P_L+\Gamma^{dR}_{iX}P_R)\tilde{G}^aT^a\tilde{d}_X\\&+\overline{u_i}(\Gamma^{uL}_{iX}P_L+\Gamma^{uR}_{iX}P_R)\tilde{G}^aT^a\tilde{u}_X\}+\text{H.c.},\end{aligned}\tag{C1}$$

where P_L and P_R are projection operators defined by $P_L=(1-\gamma_5)/2$ and $P_R=(1+\gamma_5)/2$ and T^a is the generator of the SU(3) gauge group. The neutralino-squark coupling constants appear in the above formula are given by

$$\begin{aligned}N^{dL}_{iAX}=&-\sqrt{2}g_2\left\{\frac{1}{3}\tan\theta_W(O_N)_{A1}(U^*_d)_{Xi+3}\right.\\&\left.+\frac{m_{di}}{2m_W\cos\beta}(O_N)_{A3}(U^*_d)_{Xi}\right\},\end{aligned}\tag{C2a}$$

$$\begin{aligned}N^{dR}_{iAX}=&-\sqrt{2}g_2\left[\left\{-\frac{1}{2}(O^*_N)_{A2}+\frac{1}{6}\tan\theta_W(O^*_N)_{A1}\right\}(U^*_d)_{Xi}\right.\\&\left.+\frac{m_{di}}{2m_W\cos\beta}(O_N)^*_{A3}(U^*_d)_{Xi+3}\right],\end{aligned}\tag{C2b}$$

$$\begin{aligned}N^{uL}_{iAX}=&-\sqrt{2}g_2\left\{-\frac{2}{3}\tan\theta_W(O_N)_{A1}(U^*_u)_{Xi+3}\right.\\&\left.+\sum_{j=1}^{3}\frac{m_{ui}(V_{\rm CKM})^i{}_j}{2m_W\sin\beta}(O_N)_{A3}(U^*_u)_{Xj}\right\},\end{aligned}\tag{C2c}$$

$$\begin{aligned}N^{uR}_{iAX}=&-\sqrt{2}g_2\left[\left\{\frac{1}{2}(O^*_N)_{A2}+\frac{1}{6}\tan\theta_W(O^*_N)_{A1}\right\}(U^*_u)_{Xi}\right.\\&\left.+\sum_{j=1}^{3}\frac{(V^\dagger_{\rm CKM})^i{}_jm_{uj}}{2m_W\sin\beta}(O^*_N)_{A3}(U^*_u)_{Xj+3}\right],\end{aligned}\tag{C2d}$$

where g_2 is the SU(2) gauge coupling constant. O_N is the diagonalization matrix for the neutralino mass matrix defined in Appendix B. U_d and U_u are unitary matrices that appear in diagonalization of the 6×6 squark mass matrices $m^2_{\tilde{d}}$ and $m^2_{\tilde{u}}$ as follows:

$$U_dm^2_{\tilde{d}}U^\dagger_d=\text{diag}(m^2_{\tilde{d}_1},m^2_{\tilde{d}_2},m^2_{\tilde{d}_3},m^2_{\tilde{d}_4},m^2_{\tilde{d}_5},m^2_{\tilde{d}_6}),$$

$$m^2_{\tilde{d}}=\begin{pmatrix}m^2_Q+m^\dagger_dm_d+m^2_Z\cos2\beta\left(-\frac{1}{2}+\frac{1}{3}\sin^2\theta_W\right)\mathbf{1} & \frac{v}{\sqrt{2}}\cos\beta(\tilde{y}_d+y_d\mu^*\tan\beta)^\dagger\\ \frac{v}{\sqrt{2}}\cos\beta(\tilde{y}_d+y_d\mu^*\tan\beta) & m^2_D+m_dm^\dagger_d-\frac{1}{3}m^2_Z\cos2\beta\sin^2\theta_W\mathbf{1}\end{pmatrix},\tag{C3a}$$

$$U_um^2_{\tilde{u}}U^\dagger_u=\text{diag}(m^2_{\tilde{u}_1},m^2_{\tilde{u}_2},m^2_{\tilde{u}_3},m^2_{\tilde{u}_4},m^2_{\tilde{u}_5},m^2_{\tilde{u}_6}),$$

$$m^2_{\tilde{u}}=\begin{pmatrix}m^2_Q+m^\dagger_um_u+m^2_z\cos2\beta\left(\frac{1}{2}-\frac{2}{3}\sin^2\theta_W\right)\mathbf{1} & -\frac{v}{\sqrt{2}}\sin\beta(\tilde{y}_u+y_u\mu^*\cot\beta)^\dagger\\ -\frac{v}{\sqrt{2}}\sin\beta(\tilde{y}_u+y_u\mu^*\cot\beta) & m^2_U+m_um^\dagger_u+\frac{2}{3}m^2_z\cos2\beta\sin^2\theta_W\mathbf{1}\end{pmatrix},\tag{C3b}$$

where generation indices are suppressed and the mass matrices for down-type and up-type quarks are given by $(m_d)_{ij}=m_{di}\delta^i_j$ and $(m_u)_{ij}=m_{ui}(V_{\rm CKM})^i{}_j$. The chargino-squark coupling constants in Eq. (C1) are given by

$$C^{dL}_{iAX}=g_2\frac{m_{di}}{\sqrt{2}m_W\cos\beta}(O^*_{CL})_{A2}(U^*_u)_{Xi}, \tag{C4a}$$

$$C^{dR}_{iAX}=-g_2\left\{(O^*_{CR})_{A1}(U^*_u)_{Xi}-\sum_{j=1}^{3}\frac{(V^\dagger_{\rm CKM})^i{}_j m_{uj}}{\sqrt{2}m_W\sin\beta}(O^*_{CR})_{A2}(U^*_u)_{Xj+3}\right\}, \tag{C4b}$$

$$C^{uL}_{iAX}=g_2\sum_{j=1}^{3}\frac{m_{ui}(V_{\rm CKM})^i{}_j}{\sqrt{2}m_W\cos\beta}(O_{CR})_{A2}(U^*_d)_{Xj}, \tag{C4c}$$

$$C^{uR}_{iAX}=-g_2\left\{(O_{CL})_{A1}(U^*_d)_{Xi}-\frac{m_{di}}{\sqrt{2}m_W\cos\beta}(O_{CL})_{A2}(U^*_d)_{Xi+3}\right\}, \tag{C4d}$$

where O_{CL} and O_{CR} are the diagonalization matrices for the chargino mass matrix defined in Appendix B. The gluino-squark coupling constants in Eq. (C1) are given by

$$\Gamma^{dL}_{iX}=-\sqrt{2}g_3(U^*_d)_{Xi+3}, \tag{C5a}$$

$$\Gamma^{dR}_{iX}=\sqrt{2}g_3(U^*_d)_{Xi}, \tag{C5b}$$

$$\Gamma^{uL}_{iX}=-\sqrt{2}g_3(U^*_u)_{Xi+3}, \tag{C5c}$$

$$\Gamma^{uR}_{iX}=\sqrt{2}g_3(U^*_u)_{Xi}. \tag{C5d}$$

where g_3 is the SU(3) gauge coupling constant.

The SUSY contribution to the effective FCNC coupling constants is divided into six parts as follows:

$$g=g(H^-)+g(H^-W)+g(\tilde\chi^0)+g(\tilde\chi^-)+g(\tilde G)+g(\tilde G\tilde\chi^0), \tag{C6}$$

where g represents the effective coupling constants in Eq. (37) of Sec. III B and their generalization for B^0-$\overline{B^0}$ mixing. In the following, coupling constants g are associated with indices i,j. K^0-$\overline{K^0}$ mixing corresponds to $i=1$, $j=2$ and B_d-$\overline{B_d}$ (B_s-$\overline{B_s}$) mixing corresponds to $i=1$, $j=3$ ($i=2$, $j=3$). The contribution from box diagrams including charged Higgs boson and up-type quark is given by

$$g^V_R(H^-)=-\frac{\sqrt{2}G_F}{16\pi^2}\times\sum_{k,l=1}^{3}(V^\dagger_{\rm CKM})^j{}_l(V_{\rm CKM})^l{}_i(V^\dagger_{\rm CKM})^j{}_k(V_{\rm CKM})^k{}_i\times m_{dj}{}^2m_{di}{}^2\tan^4\beta\, d_2(m^2_{H^-},m^2_{H^-},m_{uk}{}^2,m_{ul}{}^2), \tag{C7a}$$

$$g^V_L(H^-)=-\frac{\sqrt{2}G_F}{16\pi^2}\times\sum_{k,l=1}^{3}(V^\dagger_{\rm CKM})^j{}_l(V_{\rm CKM})^l{}_i(V^\dagger_{\rm CKM})^j{}_k(V_{\rm CKM})^k{}_i\times m_{ul}{}^2m_{uk}{}^2\cot^4\beta\, d_2(m^2_{H^-},m^2_{H^-},m_{uk}{}^2,m_{ul}{}^2), \tag{C7b}$$

$$g^S_{RR}(H^-)=-\frac{\sqrt{2}G_F}{16\pi^2}\times\sum_{k,l=1}^{3}(V^\dagger_{\rm CKM})^j{}_l(V_{\rm CKM})^l{}_i(V^\dagger_{\rm CKM})^j{}_k(V_{\rm CKM})^k{}_i\times m_{dj}{}^2m_{ul}{}^2m_{uk}{}^2d_0(m^2_{H^-},m^2_{H^-},m_{uk}{}^2,m_{ul}{}^2), \tag{C7c}$$

$$g^S_{LL}(H^-)=-\frac{\sqrt{2}G_F}{16\pi^2}\times\sum_{k,l=1}^{3}(V^\dagger_{\rm CKM})^j{}_l(V_{\rm CKM})^l{}_i(V^\dagger_{\rm CKM})^j{}_k(V_{\rm CKM})^k{}_i\times m_{ul}{}^2m_{uk}{}^2m_{di}{}^2d_0(m^2_{H^-},m^2_{H^-},m_{uk}{}^2,m_{ul}{}^2), \tag{C7d}$$

$$g^S_{RR}{}'(H^-)=g^S_{LL}{}'(H^-)=0, \tag{C7e}$$

$$g^S_{RL}(H^-)=-\frac{\sqrt{2}G_F}{16\pi^2}\times\sum_{k,l=1}^{3}(V^\dagger_{\rm CKM})^j{}_l(V_{\rm CKM})^l{}_i(V^\dagger_{\rm CKM})^j{}_k(V_{\rm CKM})^k{}_i\times m_{dj}m_{ul}{}^2m_{uk}{}^2m_{di}d_0(m^2_{H^-},m^2_{H^-},m_{uk}{}^2,m_{ul}{}^2), \tag{C7f}$$

$$g_{RL}^{S}{}'(H^-) = \frac{\sqrt{2}G_F}{8\pi^2} \times \sum_{k,l=1}^{3} (V_{\rm CKM}^{\dagger})^{j}{}_{l}(V_{\rm CKM})^{l}{}_{i}(V_{\rm CKM}^{\dagger})^{j}{}_{k}(V_{\rm CKM})^{k}{}_{i} \times m_{dj} m_{uk}^2 m_{di} d_2(m_{H^-}^2, m_{H^-}^2, m_{uk}^2, m_{ul}^2). \tag{C7g}$$

where m_{H^-} is the charged Higgs boson mass. The contribution from box diagrams including charged Higgs and W bosons and up-type quarks is given by

$$g_R^V(H^-W) = 0, \tag{C8a}$$

$$g_L^V(H^-W) = -\frac{\sqrt{2}G_F}{8\pi^2} \times \sum_{k,l=1}^{3} (V_{\rm CKM}^{\dagger})^{j}{}_{l}(V_{\rm CKM})^{l}{}_{i}(V_{\rm CKM}^{\dagger})^{j}{}_{k}(V_{\rm CKM})^{k}{}_{i} \times m_{ul}^2 m_{uk}^2 \cot^2\beta \{ d_2(m_{H^-}^2, m_W^2, m_{uk}^2, m_{ul}^2) - m_W^2 d_0(m_{H^-}^2, m_W^2, m_{uk}^2, m_{ul}^2) \}, \tag{C8b}$$

$$g_{RR}^S(H^-W) = g_{LL}^S(H^-W) = g_{RR}^S{}'(H^-W) = g_{LL}^S{}'(H^-W) = 0, \tag{C8c}$$

$$g_{RL}^S(H^-W) = \frac{\sqrt{2}G_F}{2\pi^2} \sum_{k,l=1}^{3} (V_{\rm CKM}^{\dagger})^{j}{}_{l}(V_{\rm CKM})^{l}{}_{i} \times (V_{\rm CKM}^{\dagger})^{j}{}_{k}(V_{\rm CKM})^{k}{}_{i} m_{dj} m_{di} m_W^2 \tan^2\beta \times \left\{ d_2(m_{H^-}^2, m_W^2, m_{uk}^2, m_{ul}^2) - \frac{m_{uk}^2 m_{ul}^2}{4m_W^2} d_0(m_{H^-}^2, m_W^2, m_{uk}^2, m_{ul}^2) \right\}, \tag{C8d}$$

$$g_{RL}^S{}'(H^-W) = 0. \tag{C8e}$$

The contribution from box diagrams including neutralinos and down-type squarks is given by

$$g_R^V(\tilde{\chi}^0) = -\frac{\sqrt{2}}{128\pi^2 G_F} \sum_{A,B=1}^{4} \sum_{X,Y=1}^{6} N_{jBY}^{dL} N_{iAY}^{dL*} \times \left\{ N_{jAX}^{dL} N_{iBX}^{dL*} d_2(m_{\tilde{\chi}_A^0}^2, m_{\tilde{\chi}_B^0}^2, m_{\tilde{d}_X}^2, m_{\tilde{d}_Y}^2) + N_{jBX}^{dL} N_{iAX}^{dL*} \frac{m_{\chi_A^0} m_{\chi_B^0}}{2} d_0(m_{\tilde{\chi}_A^0}^2, m_{\tilde{\chi}_B^0}^2, m_{\tilde{d}_X}^2, m_{\tilde{d}_Y}^2) \right\}, \tag{C9a}$$

$$g_{RR}^S(\tilde{\chi}^0) = \frac{\sqrt{2}}{128\pi^2 G_F} \sum_{A,B=1}^{4} \sum_{X,Y=1}^{6} N_{jBY}^{dR} N_{iAY}^{dL*} N_{jBX}^{dR} N_{iAX}^{dL*} \times m_{\tilde{\chi}_A^0} m_{\tilde{\chi}_B^0} d_0(m_{\tilde{\chi}_A^0}^2, m_{\tilde{\chi}_B^0}^2, m_{\tilde{d}_X}^2, m_{\tilde{d}_Y}^2), \tag{C9b}$$

$$g_{RR}^S{}'(\tilde{\chi}^0) = \frac{\sqrt{2}}{128\pi^2 G_F} \sum_{A,B=1}^{4} \sum_{X,Y=1}^{6} N_{jBY}^{dR} N_{iAY}^{dL*} \times (N_{jBX}^{dR} N_{iAX}^{dL*} - N_{jAX}^{dR} N_{iBX}^{dL*}) \times m_{\tilde{\chi}_A^0} m_{\tilde{\chi}_B^0} d_0(m_{\tilde{\chi}_A^0}^2, m_{\tilde{\chi}_B^0}^2, m_{\tilde{d}_X}^2, m_{\tilde{d}_Y}^2), \tag{C9c}$$

$$g_{RL}^S(\tilde{\chi}^0) = \frac{\sqrt{2}}{64\pi^2 G_F} \sum_{A,B=1}^{4} \sum_{X,Y=1}^{6} N_{jBY}^{dR} N_{iAY}^{dL*} (N_{jBX}^{dL} N_{iAX}^{dR*} + N_{jAX}^{dL} N_{iBX}^{dR*}) d_2(m_{\tilde{\chi}_A^0}^2, m_{\tilde{\chi}_B^0}^2, m_{\tilde{d}_X}^2, m_{\tilde{d}_Y}^2), \tag{C9d}$$

$$g_{RL}^S{}'(\tilde{\chi}^0) = -\frac{\sqrt{2}}{128\pi^2 G_F} \sum_{A,B=1}^{4} \sum_{X,Y=1}^{6} N_{jBY}^{dR} N_{iAY}^{dR*} \times \{ 2N_{jBX}^{dL} N_{iAX}^{dL*} d_2(m_{\tilde{\chi}_A^0}^2, m_{\tilde{\chi}_B^0}^2, m_{\tilde{d}_X}^2, m_{\tilde{d}_Y}^2) + N_{jAX}^{dL} N_{iBX}^{dL*} m_{\tilde{\chi}_A^0} m_{\tilde{\chi}_B^0} d_0(m_{\tilde{\chi}_A^0}^2, m_{\tilde{\chi}_B^0}^2, m_{\tilde{d}_X}^2, m_{\tilde{d}_Y}^2) \}. \tag{C9e}$$

The contribution from box diagrams including charginos and up-type squarks is given by

$$g_R^V(\tilde{\chi}^-) = -\frac{\sqrt{2}}{128\pi^2 G_F} \sum_{A,B=1}^{2} \sum_{X,Y=1}^{6} C_{jBY}^{dL} C_{iAY}^{dL*} C_{jAX}^{dL} C_{iBX}^{dL*} \times d_2(m_{\tilde{\chi}_A^-}^2, m_{\tilde{\chi}_B^-}^2, m_{\tilde{u}_X}^2, m_{\tilde{u}_Y}^2), \tag{C10a}$$

$$g_{RR}^S(\tilde{\chi}^-) = 0, \tag{C10b}$$

$$g_{RR}^S{}'(\tilde{\chi}^-) = -\frac{\sqrt{2}}{128\pi^2 G_F} \sum_{A,B=1}^{2} \sum_{X,Y=1}^{6} C_{jBY}^{dR} C_{iAY}^{dL*} C_{jAX}^{dR} C_{iBX}^{dL*} \times m_{\tilde{\chi}_A^-} m_{\tilde{\chi}_B^-} d_0(m_{\tilde{\chi}_A^-}^2, m_{\tilde{\chi}_B^-}^2, m_{\tilde{u}_X}^2, m_{\tilde{u}_Y}^2), \tag{C10c}$$

$$g_{RL}^S(\tilde{\chi}^-) = \frac{\sqrt{2}}{64\pi^2 G_F} \sum_{A,B=1}^{2} \sum_{X,Y=1}^{6} C_{jBY}^{dR} C_{iAY}^{dL*} C_{jAX}^{dL} C_{iBX}^{dR*} \times d_2(m_{\tilde{\chi}_A^-}^2, m_{\tilde{\chi}_B^-}^2, m_{\tilde{u}_X}^2, m_{\tilde{u}_Y}^2), \tag{C10d}$$

$$g_{RL}^S{}'(\tilde{\chi}^-) = -\frac{\sqrt{2}}{128\pi^2 G_F} \sum_{A,B=1}^{2} \sum_{X,Y=1}^{6} C_{jBY}^{dL} C_{iAY}^{dL*} C_{jAX}^{dR} C_{iBX}^{dR*} \times m_{\tilde{\chi}_A^-} m_{\tilde{\chi}_B^-} d_0(m_{\tilde{\chi}_A^-}^2, m_{\tilde{\chi}_B^-}^2, m_{\tilde{u}_X}^2, m_{\tilde{u}_Y}^2), \tag{C10e}$$

The contribution from box diagrams including gluinos and down-type squarks is given by

$$g_R^V(\tilde{G}) = -\frac{\sqrt{2}}{128\pi^2 G_F}\sum_{X,Y=1}^{6}\Gamma_{jY}^{dL}\Gamma_{iY}^{dL*}\Gamma_{jX}^{dL}\Gamma_{iX}^{dL*}\left\{\frac{11}{18}d_2(M_3^2,M_3^2,m_{\tilde{d}_X}^2,m_{\tilde{d}_Y}^2)+\frac{1}{18}M_3^2 d_0(M_3^2,M_3^2,m_{\tilde{d}_X}^2,m_{\tilde{d}_Y}^2)\right\}, \quad \text{(C11a)}$$

$$g_{RR}^S(\tilde{G}) = -\frac{\sqrt{2}}{128\pi^2 G_F}\sum_{X,Y=1}^{6}\frac{17}{36}\Gamma_{jY}^{dR}\Gamma_{iY}^{dL*}\Gamma_{jX}^{dR}\Gamma_{iX}^{dL*}M_3^2 d_0(M_3^2,M_3^2,m_{\tilde{d}_X}^2,m_{\tilde{d}_Y}^2), \quad \text{(C11b)}$$

$$g_{RR}^S{}'(\tilde{G}) = \frac{\sqrt{2}}{128\pi^2 G_F}\sum_{X,Y=1}^{6}\frac{1}{12}\Gamma_{jY}^{dR}\Gamma_{iY}^{dL*}\Gamma_{jX}^{dR}\Gamma_{iX}^{dL*}M_3^2 d_2(M_3^2,M_3^2,m_{\tilde{d}_X}^2,m_{\tilde{d}_Y}^2), \quad \text{(C11c)}$$

$$g_{RL}^S(\tilde{G}) = -\frac{\sqrt{2}}{128\pi^2 G_F}\sum_{X,Y=1}^{6}\left\{\left(-\frac{1}{3}\Gamma_{jY}^{dR}\Gamma_{iY}^{dR*}\Gamma_{jX}^{dL}\Gamma_{iX}^{dL*}-\frac{11}{18}\Gamma_{jY}^{dL}\Gamma_{iY}^{dR*}\Gamma_{jX}^{dR}\Gamma_{iX}^{dL*}\right)d_2(M_3^2,M_3^2,m_{\tilde{d}_X}^2,m_{\tilde{d}_Y}^2)\right.$$
$$\left.+\frac{7}{12}\Gamma_{jY}^{dL}\Gamma_{iY}^{dL*}\Gamma_{jX}^{dR}\Gamma_{iX}^{dR*}M_3^2 d_0(M_3^2,M_3^2,m_{\tilde{d}_X}^2,m_{\tilde{d}_Y}^2)\right\}, \quad \text{(C11d)}$$

$$g_{RL}^S{}'(\tilde{G}) = -\frac{\sqrt{2}}{128\pi^2 G_F}\sum_{X,Y=1}^{6}\left\{\left(-\frac{5}{6}\Gamma_{jY}^{dL}\Gamma_{iY}^{dR*}\Gamma_{jX}^{dR}\Gamma_{iX}^{dL*}+\frac{5}{9}\Gamma_{jY}^{dR}\Gamma_{iY}^{dR*}\Gamma_{jX}^{dL}\Gamma_{iX}^{dL*}\right)\times d_2(M_3^2,M_3^2,m_{\tilde{d}_X}^2,m_{\tilde{d}_Y}^2)\right.$$
$$\left.+\frac{1}{36}\Gamma_{jY}^{dL}\Gamma_{iY}^{dL*}\Gamma_{jX}^{dR}\Gamma_{iX}^{dR*}M_3^2 d_0(M_3^2,M_3^2,m_{\tilde{d}_X}^2,m_{\tilde{d}_Y}^2)\right\}. \quad \text{(C11e)}$$

The contribution from box diagrams including neutralinos, gluinos, and down-type squarks is given by

$$g_R^V(\tilde{G}\tilde{\chi}^0) = -\frac{\sqrt{2}}{128\pi^2 G_F}\sum_{A=1}^{4}\sum_{X,Y=1}^{6}\left\{\frac{2}{3}N_{jAY}^{dL}\Gamma_{iY}^{dL*}\Gamma_{jX}^{dL}N_{iAX}^{dL*}d_2(m_{\tilde{\chi}_A^0}^2,M_3^2,m_{\tilde{d}_X}^2,m_{\tilde{d}_Y}^2)\right.$$
$$\left.+\frac{1}{6}(N_{jAY}^{dL}\Gamma_{iY}^{dL*}N_{jAX}^{dL}\Gamma_{iX}^{dL*}+\Gamma_{jY}^{dL}N_{iAY}^{dL*}\Gamma_{jX}^{dL}N_{iAX}^{dL*})\times m_{\tilde{\chi}_A^0}M_3 d_0(m_{\tilde{\chi}_A^0}^2,M_3^2,m_{\tilde{d}_X}^2,m_{\tilde{d}_Y}^2)\right\}, \quad \text{(C12a)}$$

$$g_{RR}^S(\tilde{G}\tilde{\chi}^0) = -\frac{\sqrt{2}}{128\pi^2 G_F}\sum_{A=1}^{4}\sum_{X,Y=1}^{6}\left\{N_{jAY}^{dR}\Gamma_{iY}^{dL*}\Gamma_{jX}^{dR}N_{iAX}^{dL*}-\frac{1}{3}(N_{jAY}^{dR}\Gamma_{iY}^{dL*}N_{jAX}^{dR}\Gamma_{iX}^{dL*}+\Gamma_{jY}^{dR}N_{iAY}^{dL*}\Gamma_{jX}^{dR}N_{iAX}^{dL*})\right\}$$
$$\times m_{\tilde{\chi}_A^0}M_3 d_0(m_{\tilde{\chi}_A^0}^2,M_3^2,m_{\tilde{d}_X}^2,m_{\tilde{d}_Y}^2), \quad \text{(C12b)}$$

$$g_{RR}^S{}'(\tilde{G}\tilde{\chi}^0) = \frac{\sqrt{2}}{128\pi^2 G_F}\sum_{A=1}^{4}\sum_{X,Y=1}^{6}\frac{1}{3}(N_{jAY}^{dR}\Gamma_{iY}^{dL*}\Gamma_{jX}^{dR}N_{iAX}^{dL*}+N_{jAY}^{dR}\Gamma_{iY}^{dL*}N_{jAX}^{dR}\Gamma_{iX}^{dL*}+\Gamma_{jY}^{dR}N_{iAY}^{dL*}\Gamma_{jX}^{dR}N_{iAX}^{dL*})$$
$$\times m_{\tilde{\chi}_A^0}M_3 d_0(m_{\tilde{\chi}_A^0}^2,M_3^2,m_{\tilde{d}_X}^2,m_{\tilde{d}_Y}^2), \quad \text{(C12c)}$$

$$g_{RL}^S(\tilde{G}\tilde{\chi}^0) = -\frac{\sqrt{2}}{128\pi^2 G_F}\sum_{A=1}^{4}\sum_{X,Y=1}^{6}\left[\left\{\frac{1}{3}(N_{jAY}^{dL}\Gamma_{iY}^{dR*}+\Gamma_{jY}^{dL}N_{iAY}^{dR*})(\Gamma_{jX}^{dR}N_{iAX}^{dL*}+N_{jAX}^{dR}\Gamma_{iX}^{dL*})\right.\right.$$
$$\left.+(N_{jAY}^{dR}\Gamma_{iY}^{dR*}N_{jAX}^{dL}\Gamma_{iX}^{dL*}+\Gamma_{jY}^{dR}N_{iAY}^{dR*}\Gamma_{jX}^{dL}N_{iAX}^{dL*})\right\}d_2(m_{\tilde{\chi}_A^0}^2,M_3^2,m_{\tilde{d}_X}^2,m_{\tilde{d}_Y}^2)$$
$$\left.+\frac{1}{2}(N_{jAY}^{dL}\Gamma_{iY}^{dL*}\Gamma_{jX}^{dR}N_{iAX}^{dR*}+\Gamma_{jY}^{dL}N_{iAY}^{dL*}N_{jAX}^{dR}\Gamma_{iX}^{dR*})m_{\tilde{\chi}_A^0}M_3 d_0(m_{\tilde{\chi}_A^0}^2,M_3^2,m_{\tilde{d}_X}^2,m_{\tilde{d}_Y}^2)\right], \quad \text{(C12d)}$$

$$g_{RL}^{S}{}'(\tilde{G}\tilde{\chi}^0)=\frac{\sqrt{2}}{128\pi^2 G_F}\sum_{A=1}^{4}\sum_{X,Y=1}^{6}\Bigg[\Bigg\{(N_{jAY}^{dL}\Gamma_{iY}^{dR*}+\Gamma_{jY}^{dL}N_{iAY}^{dR*})(N_{jAX}^{dR}\Gamma_{iX}^{dL*}+\Gamma_{jX}^{dR}N_{iAX}^{dL*})$$
$$+\frac{1}{3}(N_{jAY}^{dR}\Gamma_{iY}^{dR*}N_{jAX}^{dL}\Gamma_{iX}^{dL*}+\Gamma_{jY}^{dR}N_{iAY}^{dR*}\Gamma_{jX}^{dL}N_{iAX}^{dL*})\Bigg\}d_2(m_{\tilde{\chi}_A^0}^2,M_3^2,m_{\tilde{d}_X}^2,m_{\tilde{d}_Y}^2)+\frac{1}{6}(N_{jAY}^{dL}\Gamma_{iY}^{dL*}\Gamma_{jX}^{dR}N_{iAX}^{dR*}$$
$$+\Gamma_{jY}^{dL}N_{iAY}^{dL*}N_{jAX}^{dR}\Gamma_{iX}^{dR*})M_3 m_{\tilde{\chi}_A^0}d_0(m_{\tilde{\chi}_A^0}^2,M_3^2,m_{\tilde{d}_X}^2,m_{\tilde{d}_Y}^2)\Bigg], \tag{C12e}$$

The neutralino, chargino, gluino, and neutralino-gluino contributions to g_L^V, g_{LL}^S, and $g_{LL}^S{}'$ are obtained by replacing the suffix R with L and L with R in the corresponding formulas for g_R^V, g_{RR}^S, and $g_{RR}^S{}'$, respectively. The mass functions that appear in the above formulas are defined as follows:

$$d_0(x,y,z,w)=\frac{x\ln(x)}{(y-x)(z-x)(w-x)}+\frac{y\ln(y)}{(x-y)(z-y)(w-y)}+\frac{z\ln(z)}{(x-z)(y-z)(w-z)}+\frac{w\ln(w)}{(x-w)(y-w)(z-w)}, \tag{C13a}$$

$$d_2(x,y,z,w)=\frac{1}{4}\left\{\frac{x^2\ln(x)}{(y-x)(z-x)(w-x)}+\frac{y^2\ln(y)}{(x-y)(z-y)(w-y)}+\frac{z^2\ln(z)}{(x-z)(y-z)(w-z)}+\frac{w^2\ln(w)}{(x-w)(y-w)(z-w)}\right\}. \tag{C13b}$$

[1] Muon $g-2$ Collaboration, H.N. Brown *et al.*, Phys. Rev. Lett. **86**, 2227 (2001).

[2] J. Ellis and D.V. Nanopoulos, Phys. Lett. **110B**, 44 (1982); R. Barbieri and R. Gatto, *ibid.* **110B**, 211 (1982); T. Inami and C.S. Lim, Nucl. Phys. **B207**, 533 (1982).

[3] M.J. Duncan, Nucl. Phys. **B221**, 285 (1983); J.F. Donoghue, H.P. Nilles, and D. Wyler, Phys. Lett. **128B**, 55 (1983); A. Bouquet, J. Kaplan, and C.A. Savoy, *ibid.* **148B**, 69 (1984).

[4] L.J. Hall, V.A. Kostelecky, and S. Raby, Nucl. Phys. **B267**, 415 (1986).

[5] T. Kurimoto, Phys. Rev. D **39**, 3447 (1989); G.C. Branco, G.C. Cho, Y. Kizukuri, and N. Oshimo, Phys. Lett. B **337**, 316 (1994).

[6] S. Bertolini, F. Borzumati, A. Masiero, and G. Ridolfi, Nucl. Phys. **B353**, 590 (1991).

[7] T. Goto, T. Nihei, and Y. Okada, Phys. Rev. D **53**, 5233 (1996); **54**, 5904(E) (1996); T. Goto, Y. Okada, and Y. Shimizu, *ibid.* **58**, 094006 (1998).

[8] T. Goto, Y. Okada, and Y. Shimizu, KEK Report No. 99-72, KEK-TH-611, hep-ph/9908499.

[9] F. Gabbiani and A. Masiero, Nucl. Phys. **B322**, 235 (1989); J.S. Hagelin, S. Kelley, and T. Tanaka, *ibid.* **B415**, 293 (1994).

[10] R. Barbieri and L.J. Hall, Phys. Lett. B **338**, 212 (1994); R. Barbieri, L. Hall, and A. Strumia, Nucl. Phys. **B445**, 219 (1995).

[11] R. Barbieri, L. Hall, and A. Strumia, Nucl. Phys. **B449**, 437 (1995); N.G. Deshpande, B. Dutta, and S. Oh, Phys. Rev. Lett. **77**, 4499 (1996).

[12] P. Ciafaloni, A. Romanino, and A. Strumia, Nucl. Phys. **B458**, 3 (1996); N. Arkani-Hamed, H. Cheng, and L.J. Hall, Phys. Rev. D **53**, 413 (1996); T.V. Duong, B. Dutta, and E. Keith, Phys. Lett. B **378**, 128 (1996); M.E. Gómez and H. Goldberg, Phys. Rev. D **53**, 5244 (1996); N.G. Deshpande, B. Dutta, and E. Keith, *ibid.* **54**, 730 (1996); J. Hisano, T. Moroi, K. Tobe, and M. Yamaguchi, Phys. Lett. B **391**, 341 (1997); **397**, 357(E) (1997); J. Hisano, D. Nomura, Y. Okada, Y. Shimizu, and M. Tanaka, Phys. Rev. D **58**, 116010 (1998); G. Barenboim, K. Huitu, and M. Raidal, *ibid.* **63**, 055006 (2001).

[13] Super-Kamiokande Collaboration, Y. Fukuda *et al.*, Phys. Rev. Lett. **81**, 1562 (1998); E. Kearns, talk at the 30th International Conference on High Energy Physics (ICHEP 2000), Osaka, 2000.

[14] T. Yanagida, in Proceedings of the Workshop on Unified Theory and Baryon Number of the Universe, Tsukuba, Japan, 1979, edited by O. Sawada and A. Sugamoto; M. Gell-Mann, P. Ramond, and R. Slansky, in *Supergravity*, edited by P. van Nieuwenhuizen and D. Freedman (North-Holland, Amsterdam, 1979).

[15] F. Borzumati and A. Masiero, Phys. Rev. Lett. **57**, 961 (1986); J. Hisano, T. Moroi, K. Tobe, M. Yamaguchi, and T. Yanagida, Phys. Lett. B **357**, 579 (1995); J. Hisano, T. Moroi, K. Tobe, and M. Yamaguchi, Phys. Rev. D **53**, 2442 (1996); J.A. Casas and A. Ibarra, hep-ph/0103065.

[16] J. Hisano, D. Nomura, and T. Yanagida Phys. Lett. B **437**, 351 (1998).

[17] J. Hisano and D. Nomura, Phys. Rev. D **59**, 116005 (1999).

[18] M.E. Gómez, G.K. Leontaris, S. Lola, and J.D. Vergados, Phys. Rev. D **59**, 116009 (1999); W. Buchmuller, D. Delepine, and F. Vissani, Phys. Lett. B **459**, 171 (1999); J. Ellis, M.E. Gómez, G.K. Leontaris, S. Lola, and D.V. Nanopoulos, Eur. Phys. J. C **14**, 319 (2000); W. Buchmuller, D. Delepine, and L.T. Handoko, Nucl. Phys. **B576**, 445 (2000); J.L. Feng, Y. Nir, and Y. Shadmi, Phys. Rev. D **61**, 113005 (2000); J. Sato, K. Tobe, and T. Yanagida, Phys. Lett. B **498**, 189 (2001); J. Sato and K. Tobe, Phys. Rev. D **63**, 116010 (2001).

[19] S. Baek, T. Goto, Y. Okada, and K. Okumura, Phys. Rev. D **63**, 051701(R) (2001); talk at the 30th International Conference on High-Energy Physics (ICHEP 2000), Osaka, 2000, hep-ph/0009196.

[20] T. Moroi, J. High Energy Phys. **03**, 019 (2000); Phys. Lett. B **493**, 366 (2000).

[21] A. Czarnecki and W.J. Marciano, Phys. Rev. D **64**, 013014 (2001); L. Everett, G.L. Kane, S. Rigolin, and L.-T. Wang, Phys. Rev. Lett. **86**, 3484 (2001); J.L. Feng and K. Matchev, *ibid.* **86**, 3480 (2001); E.A. Baltz and P. Gondolo, *ibid.* **86**, 5004 (2001); U. Chattopadhyay and P. Nath, *ibid.* **86**, 5854 (2001); R. Arnowitt, B. Dutta, B. Hu, and Y. Santoso, Phys. Lett. B **505**, 177 (2001); S. Komine, T. Moroi, and M. Yamaguchi, Phys. Lett. B **506**, 93 (2001); J. Hisano and K. Tobe, hep-ph/0102315; T. Ibrahim, U. Chattopadhyay, and P. Nath, Phys. Rev. D **64**, 016010 (2001); J. Ellis, D.V. Nanopoulos, and K.A. Olive, hep-ph/0102331; K. Choi, K. Hwang, S. K. Kang, K. Y. Lee, and W. Y. Song, Phys. Rev. D **64**, 055001 (2001); S. Narison, Phys. Lett. B (to be published); S. Baek, P. Ko, and H.S. Lee, hep-ph/0103218; D.F. Carvalho, J. Ellis, M.E. Gómez, and S. Lola, hep-ph/0103256; H. Baer, C. Balázs, J. Ferrandis, and X. Tata, Phys. Rev. D **64**, 035004 (2001).

[22] Z. Maki, M. Nakagawa, and S. Sakata, Prog. Theor. Phys. **28**, 870 (1962).

[23] CHOOZ Collaboration, M. Apollonio *et al.*, Phys. Lett. B **466**, 466 (1999).

[24] P. Fayet, in *Unification of the Fundamental Particle Interactions*, edited by S. Ferrara, J. Ellis, and P. van Nieuwenhuizen (Plenum, New York, 1980), p. 587; J.A. Grifols and A. Mendez, Phys. Rev. D **26**, 1809 (1982); J. Ellis, H.S. Hagelin, and D.V. Nanopoulos, Phys. Lett. **116B**, 283 (1982); R. Barbieri and L. Maiani, *ibid.* **117B**, 203 (1982); D.A. Kosower, L.M. Krauss, and N. Sakai, *ibid.* **133B**, 305 (1983); T.C. Yuan, R. Arnowitt, A.H. Chamseddine, and P. Nath, Z. Phys. C **26**, 407 (1984); T. Moroi, Phys. Rev. D **53**, 6565 (1996).

[25] J. Lopez, D.V. Nanopoulos, and X. Wang, Phys. Rev. D **49**, 366 (1994); U. Chattopadhyay and P. Nath, *ibid.* **53**, 1648 (1996).

[26] Y. Okada, K. Okumura, and Y. Shimizu, Phys. Rev. D **61**, 094001 (2000).

[27] R. Kitano and Y. Okada, Phys. Rev. D **63**, 113003 (2001).

[28] D. Atwood, M. Gronau, and A. Soni, Phys. Rev. Lett. **79**, 185 (1997); C. Chua, X. He, and W. Hou, Phys. Rev. D **60**, 014003 (1999).

[29] A.J. Buras, M. Jamin, and P.H. Weisz, Nucl. Phys. **B347**, 491 (1990); I.I. Bigi and F. Gabbiani, *ibid.* **B352**, 309 (1991); S. Herrlich and U. Nierste, *ibid.* **B419**, 292 (1994); **B476**, 27 (1996); J. Urban, F. Krauss, U. Jentschura, and G. Soff, *ibid.* **B523**, 40 (1998).

[30] CDF Collaboration F. Abe *et al.*, Phys. Rev. D **56**, 1357 (1997); D0 Collaboration, S. Abachi *et al.*, Phys. Rev. Lett. **75**, 618 (1995); ALEPH Collaboration, R. Barate *et al.*, Phys. Lett. B **499**, 67 (2001).

[31] ALEPH Collaboration, R. Barate *et al.*, Phys. Lett. B **499**, 53 (2001); L3 Collaboration, M. Acciarri *et al.*, *ibid.* **503**, 21 (2001); DELPHI Collaboration, P. Abreu *et al.*, *ibid.* **499**, 23 (2001); OPAL Collaboration, G. Abbiendi *et al.*, *ibid.* **499**, 38 (2001).

[32] CLEO Collaboration, T. Coan, talk at the 30th International Conference on High-Energy Physics (ICHEP 2000), Osaka, 2000; Belle Collaboration, A. Abashian *et al.*, KEK Report No. 2001-3, BELLE Report No. 2001-2, hep-ex/0103042.

[33] L. Chau and W. Keung, Phys. Rev. Lett. **53**, 1802 (1984).

[34] MEGA Collaboration, M.L. Brooks *et al.*, Phys. Rev. Lett. **83**, 1521 (1999).

[35] Belle Collaboration, A. Abashian *et al.*, Phys. Rev. Lett. **86**, 2509 (2001); BaBar Collaboration, B. Aubert *et al.*, *ibid.* **86**, 2515 (2001).

[36] N. Yamada, S. Hashimoto, K. Ishikawa, H. Matsufuru, and T. Onogi, Nucl. Phys. B (Proc. Suppl.) **83**, 340 (2000); JLQCD Collaboration, S. Aoki *et al.*, Phys. Rev. D **60**, 034511 (1999); R. Gupta, T. Bhattacharya, and S. Sharpe, *ibid.* **55**, 4036 (1997); M. Ciuchini *et al.*, J. High Energy Phys. **10**, 008 (1998); CP-PACS Collaboration, A. Ali Khan *et al.*, Nucl. Phys. B (Proc. Suppl.) **83**, 265 (2000).

[37] CDF Collaboration, T. Affolder *et al.*, Phys. Rev. D **61**, 072005 (2000).

[38] T. Goto and T. Nihei, Phys. Rev. D **59**, 115009 (1999); K.S. Babu and M.J. Strassler, hep-ph/9808447; T. Goto and T. Nihei, in Proceedings of the KIAS-CTP International Symposium on Supersymmetry, Supergravity and Superstring, Seoul, Korea, 1999, edited by J. E. Kim and C. Lee.

[39] J. Hisano, H. Murayama, and T. Yanagida, Phys. Lett. B **291**, 263 (1992); K.S. Babu and S.M. Barr, Phys. Rev. D **48**, 5354 (1993); J. Hisano, T. Moroi, K. Tobe, and T. Yanagida, Phys. Lett. B **342**, 138 (1995); K.S. Babu and S.M. Barr, Phys. Rev. D **51**, 2463 (1995).

[40] Y. Kuno and Y. Okada, Rev. Mod. Phys. **73**, 151 (2001).

[41] A. Czarnecki, W.J. Marciano, and K. Melnikov, in *Workshop on Physics at the First Muon Collider and at the Front End of the Muon Collider*, edited by S. H. Geer and R. Raja, AIP Conf. Proc. No. 435 (AIP, Woodbury, NY, 1998), p. 409.

[42] P.G. Harris *et al.*, Phys. Rev. Lett. **82**, 904 (1999).

[43] E.D. Commins *et al.*, Phys. Rev. A **50**, 2960 (1994).

[44] L. M. Barkov *et al.*, "Search for the Decay $\mu^+ \rightarrow e^+ \gamma$ Down to 10^{-14} Branching Ratio," Research Proposal to Paul Scherrer Institut, 1999.

[45] MECO Collaboration, M. Bachman *et al.*, "A Search for $\mu^- N \rightarrow e^- N$ with Sensitivity Below 10^{-16}," Experimental Proposal E940 to Brookhaven National Laboratory, AGS, 1997.